PAPER SP 18-10 An extensive laboratory investigation of plain and reinforced concrete members subjected to torsion is being reported in a series of papers. This paper reports tests of 53 reinforced concrete beams which were subjected to pure torsion to investigate the effect of eight variables. The behavior before and after cracking was extensively studied. Provisions of foreign codes and theories for reinforced concrete design in torsion were evaluated. Design equations for ultimate torque, cracking torque, stiffness before and after cracking, angle of twist at ultimate torque, and at cracking torque and other provisions are given.

Torsion of Structural Concrete—Behavior of Reinforced Concrete Rectangular Members

By THOMAS T. C. HSU

□ Experimental and theoretical studies of structural concrete members subject to torsion began at the PCA Laboratories in 1962. A torsion test rig[1] was designed and constructed for a maximum torque of one million in.-lb to accommodate test beams up to 15 x 20 in. Three types of tests have so far been completed, all involving rectangular members subjected to pure torsion only: (1) plain concrete members, (2) reinforced concrete members, and (3) plain and reinforced hollow members. Future investigations will concern nonrectangular cross-sections (L-, T-, and I-beams) and members subjected to combined torsion, bending, and shear.

TORSIONAL STRENGTH OF PLAIN CONCRETE

The investigation of plain concrete rectangular members is reported in Reference 2 (see Paper SP 18-8 herein). It was found that plain concrete rectangular members subjected to torsion fail mainly by bending about an axis parallel to the wider cross-section face and inclined at 45 deg to the longitudinal axis. Based on this failure mechanism, new expressions for the ultimate torque were derived:

$$T_{up} = 2\ (x^2 + 10)\ y\ \sqrt[3]{f_t^{\,2}} \qquad (1)$$

THOMAS T. C. HSU is a Development Engineer in the Portland Cement Association Research and Development Division. For biographical sketch, see Paper SP 18-6.

where

T_{up} = ultimate torque of plain concrete members, in.-lb

x = smaller dimension of cross-section, in.

y = larger dimension of cross-section, in.

f_t = uniaxial tensile strength of concrete, psi

When only the cylinder compressive strength, f'_c, is known, f_t can be taken as $5\sqrt{f'_c}$ and Eq. (1) becomes.

$$T_{up} = 6\ (x^2 + 10)\ y\ \sqrt[3]{f'_c} \tag{1a}$$

The angle of twist at failure was found to be

$$\theta_{up} = \frac{0.0038}{\beta\, x}\left(1 + \frac{10}{x^2}\right) \tag{2}$$

in which

θ_{up} = angle of twist at failure of plain concrete members, expressed in deg/in.

β = coefficient given by Saint-Venant's theory as a function of y/x.

The investigation of plain concrete rectangular members was accompanied by an investigation of reinforced concrete rectangular members. The behavior of the reinforced rectangular members is the subject of this paper.

TESTS OF REINFORCED RECTANGULAR BEAMS

To study the behavior under pure torsion of reinforced concrete beams with rectangular cross-sections, 53 beams were tested, involving the following eight major variables:

(1) Amount of reinforcement

(2) Solid beams versus hollow beams

(3) Ratio of volume of longitudinal bars to volume of stirrups

(4) Concrete strength

(5) Scale effects

(6) Depth-to-width ratio of cross-section

(7) Spacing of longitudinal bars

(8) Spacing of stirrups.

Nine series of beams were tested as outlined in Table 10-1. Only one type of reinforcing steel, intermediate grade, was used in this investigation.

TABLE 10-1 OUTLINE OF TEST PROGRAM

Beam Series	Cross-Section in. x in.	Target f'_c psi	m	Variables Isolated							
				p_t	Solid Versus Hollow	m	f'_c	Scale Effect	$\frac{y}{x}$	Spacing, Longitudinal Bars	Spacing, Stirrups
B	10 x 15	4000	0.205-4.97	o	x	x	x		x		o
D	10 x 15 hollow	4000	1.0	o	x						o
M	10 x 15	4000	1.5	o		x					o
I	10 x 15	6500	1.0	o			x				o
J	10 x 15	2000	1.0	o			x				o
G	10 x 20	4000	1.0	o				x	x	o	o
N	6 x 12	4000	1.0	o				x	x	o	o
K	6 x 19.5	4000	1.0	o					x		o
C	10 x 10	4000	1.0	o					x		o

Note: o = comparison within each series; x = comparison between series.

Test Specimens

A typical test beam is shown in Fig. 10-1. The length of all beams was 122 in., except those of Series N. A length of 14 in. at each end of the beam was threaded into the clamping heads of the torsion test rig, through which the torsional moments were applied. The clear span subjected to torsion was 94 in. To avoid local failure close to the clamping heads due to stress concentration, a length of 25 in. at each end of the beams was reinforced with about 30 percent additional stirrups. The effective length of each beam was therefore reduced to about 72 in. The cross-sections used in each beam series are shown in Fig. 10-2.

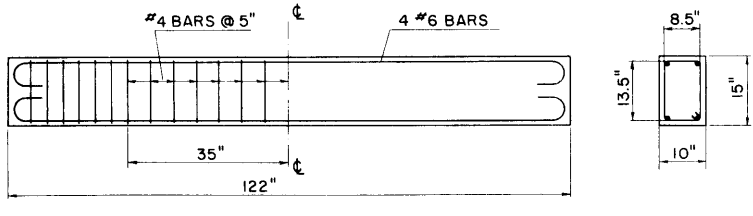

FIG. 10-1 TYPICAL TEST BEAM, B3

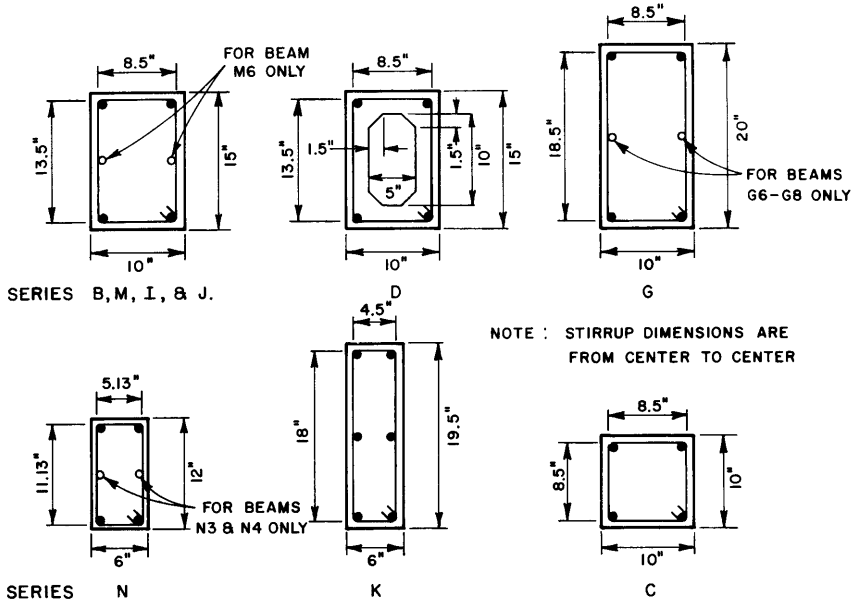

FIG. 10-2 CROSS-SECTIONS OF TEST BEAMS

The beams of Series N, with a length of 86 in. instead of 122 in., were 3/5 the scale of the beams in Series G. The clear span subjected to torsion was 58 in., and the effective length of the beams was 43 in.

As shown in Fig. 10-2, the beams of Series D were hollow. A length of 14 in. at each end of the beams was solid, however, to prevent crushing of the wall by the clamping heads of the test rig.

Reinforcement

All reinforcement was intermediate grade deformed bars having yield strengths from 45 ksi to 52 ksi as listed in Table 10-2. The yield strength of most steel was close to 48.5 ksi. The bar deformations conformed to ASTM Designation A305, and the No. 2 bars were similarly deformed. A typical stress-strain curve for the reinforcement is shown in Fig. 10-3. The modulus of elasticity was about 28.5 million psi.

The reinforcing cages for the beams usually consisted of four longitudinal corner bars and closed stirrups tied together by soft steel wire. In Beams G6-G8, N3-N4, K1-K4, and M6, however, two additional longitudinal bars were placed at the center of each wider face. The stirrups were distributed uniformly both within and outside the effective length. Details of reinforcement for each beam are listed in Table 10-2.

TABLE 10-2 REINFORCEMENT

Beam	$f_{\ell y}$ ksi	f_{sy} ksi	Longit. Bars	p_ℓ %	Stirrups Bar s, in.	p_s %	m	p_t %
B1	45.5	49.5	4 #4	0.534	#3 at 6	0.537	1.00	1.07
B2	45.9	46.4	4 #5	0.827	#4 at 7 1/8	0.823	1.00	1.65
B3	47.5	46.4	4 #6	1.17	#4 at 5	1.17	1.00	2.34
B4	46.4	46.9	4 #7	1.60	#4 at 3 5/8	1.61	0.99	3.21
B5	48.2	46.6	4 #8	2.11	#4 at 2 3/4	2.13	0.99	4.24
B6	48.1	46.8	4 #9	2.67	#4 at 2 1/4	2.61	1.02	5.28
B7	46.4	46.2	4 #4	0.534	#4 at 5	1.17	0.456	1.70
B8	46.7	46.4	4 #4	0.534	#4 at 2 1/4	2.61	0.205	3.14
B9	46.3	49.7	4 #6	1.17	#3 at 6	0.537	2.18	1.71
B10	48.5	49.6	4 #9	2.67	#3 at 6	0.537	4.97	3.21
D1	48.3	49.0	4 #4	0.534	#3 at 6	0.537	1.00	1.07
D2	46.8	48.0	4 #5	0.827	#4 at 7 1/8	0.823	1.00	1.65
D3	49.5	48.3	4 #6	1.17	#4 at 5	1.17	1.00	2.34
D4	47.9	48.3	4 #7	1.60	#4 at 3 5/8	1.61	0.99	3.21
M1	47.3	51.2	4 #5	0.827	#3 at 5 7/8	0.549	1.51	1.38
M2	47.7	51.8	4 #6	1.17	#3 at 4 1/8	0.781	1.50	1.95
M3	46.7	47.3	4 #7	1.60	#4 at 5 1/2	1.07	1.50	2.67
M4	46.2	47.4	4 #8	2.11	#4 at 4 1/8	1.42	1.49	3.53
M5	48.6	48.0	4 #9	2.67	#4 at 3 1/4	1.81	1.48	4.48
M6	46.1	49.4	6 #8	3.16	#4 at 2 3/4	2.13	1.48	5.29
I2	47.2	50.6	4 #5	0.827	#3 at 3 7/8	0.832	0.99	1.66
I3	49.8	48.4	4 #6	1.17	#4 at 5	1.17	1.00	2.34
I4	45.7	47.3	4 #7	1.60	#4 at 3 5/8	1.61	0.99	3.21
I5	45.0	47.2	4 #8	2.11	#4 at 2 3/4	2.13	0.99	4.24
I6	47.2	47.7	4 #9	2.67	#4 at 2 1/4	2.61	1.02	5.28
J1	47.5	50.2	4 #4	0.534	#3 at 6	0.537	1.00	1.07
J2	46.4	49.4	4 #5	0.827	#3 at 3 7/8	0.832	0.99	1.66
J3	49.1	48.9	4 #6	1.17	#4 at 5	1.17	1.00	2.34
J4	47.0	48.1	4 #7	1.60	#4 at 3 5/8	1.61	0.99	3.21
G1	46.7	49.2	4 #4	0.400	#3 at 7 3/8	0.402	1.00	0.802
G2	46.8	48.4	4 #5	0.620	#3 at 4 3/4	0.626	0.99	1.25
G3	49.1	47.5	4 #6	0.880	#4 at 6 1/8	0.882	1.00	1.76
G4	47.2	46.6	4 #7	1.20	#4 at 4 1/2	1.20	1.00	2.40
G5	48.0	47.5	4 #8	1.58	#4 at 3 3/8	1.60	0.99	3.18
G6	48.5	50.7	6 #4	0.600	#3 at 5	0.594	1.01	1.19
G7	46.3	46.8	6 #5	0.930	#4 at 5 3/4	0.938	0.99	1.87
G8	46.7	47.7	6 #6	1.32	#4 at 4 1/8	1.31	1.01	2.63
N1	51.1	49.5	4 #3	0.611	#2 at 3 5/8	0.622	0.98	1.23
N1a	50.2	50.0	4 #3	0.611	#2 at 3 5/8	0.622	0.98	1.23
N2	48.0	49.0	4 #4	1.11	#2 at 2	1.13	0.98	2.24
N2a	48.3	52.3	4 #4	1.11	#3 at 4 1/2	1.10	1.01	2.21
N3	51.0	51.0	6 #3	0.916	#2 at 2 1/2	0.903	1.01	1.82
N4	48.9 / 50.5	51.6	4 #4 / 2 #3	1.42	#3 at 3 1/2	1.42	1.00	2.84
K1	50.1	51.4	6 #3	0.564	#3 at 7 1/2	0.565	1.00	1.13
K2	48.7	49.0	6 #4	1.025	#3 at 4 1/8	1.027	1.00	2.05
K3	45.8	46.5	6 #5	1.59	#4 at 4 7/8	1.58	1.01	3.17
K4	49.9	49.3	6 #6	2.26	#4 at 3 3/8	2.28	0.99	4.54
C1	49.5	49.5	4 #3	0.440	#3 at 8 1/2	0.440	1.00	0.88
C2	48.5	50.0	4 #4	0.800	#3 at 4 5/8	0.808	0.99	1.61
C3	48.0	47.8	4 #5	1.24	#4 at 5 1/2	1.24	1.00	2.48
C4	48.8	47.5	4 #6	1.76	#4 at 3 7/8	1.76	1.00	3.52
C5	47.6	47.7	4 #7	2.40	#4 at 2 7/8	2.36	1.01	4.77
C6	45.8	47.5	4 #8	3.16	#4 at 2 1/8	3.20	0.99	6.36

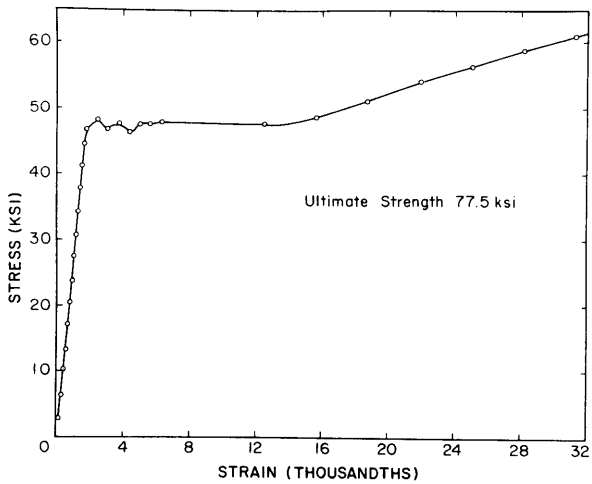

FIG. 10-3 STRESS-STRAIN CURVE OF A TYPICAL NO. 4 BAR

Concrete

The concrete mixture used in this investigation was the 1:3.5:4 mixture reported in Reference 2, except that for Series I and J the proportions were 1:2.5:4 and 1:4.5:6, respectively. Plastic-coated plywood forms were used for the torsion beams, and steel molds for the companion 6 x 12-in. cylinders. All specimens were cured four days under polyethylene sheets in the forms and then stripped and stored at 70 F and 50 percent relative humidity until tested at age 11 to 14 days.

Strength properties of the concretes are given in Table 10-3. The test methods for split-cylinder strength and direct tensile strength are reported in Reference 2. The modulus of rupture was obtained by third-point loading of 6 by 6-in. beams with a span of 18 in.

Torsion Test

Torsion beams were tested in a specially designed torsion test rig.[1] The torques were monitored by two SR4-gage tensile load cells, and the angle of twist was measured by a Metrisite differential transformer. The length of beam over which the angle of twist was measured was 53 in. for all beams except Series N, for which 32 in. was used. The testing details were reported in Reference 1. The principal test results of torque, angle of twist, and stiffness are listed in Table 10-4.

Strains in the reinforcement were measured by Type A-12 SR4 gages of 1-in. length. Four gages were mounted on the corner

TABLE 10-3 CONCRETE PROPERTIES

Beam	f'_c psi	f_{sp} psi	f_r psi	f_t psi		
				Vert. Cast	Horiz. Cast	Avg.
B1	4000	472	-	-	-	-
B2	4150	454	-	353	410	381
B3	4070	409	-	334	-	-
B4	4430	456	-	380	426	403
B5	4210	434	-	369	-	-
B6	4180	508	-	373	359	366
B7	3770	372	-	-	-	-
B8	3880	446	-	336	341	338
B9	4180	472	-	322	383	353
B10	3840	458	-	330	336	333
D1	3860	398	510	390	411	403
D2	3710	448	509	350	386	368
D3	4120	467	488	375	367	371
D4	4440	454	531	357	390	374
M1	4330	441	598	-	-	-
M2	4430	475	615	364	362	363
M3	3880	448	516	354	367	361
M4	3850	423	537	350	361	356
M5	4060	474	550	377	412	394
M6	4260	456	545	378	374	376
I2	6560	599	670	-	474	-
I3	6490	598	611	445	450	448
I4	6520	669	615	458	-	-
I5	6530	610	663	473	-	-
I6	6640	572	652	455	445	450
J1	2080	298	402	228	220	224
J2	2110	289	370	236	237	237
J3	2450	368	484	246	276	261
J4	2430	328	427	237	242	240
G1	4320	456	-	351	381	366
G2	4480	545	543	370	443	406
G3	3890	457	523	374	386	380
G4	4100	446	-	368	381	375
G5	3900	455	-	355	380	368
G6	4340	-	518	380	383	381
G7	4490	523	588	400	388	394
G8	4110	-	517	356	347	370
N1	4280	470	-	366	377	371
N1a	4160	470	-	-	-	-
N2	4410	488	-	375	366	370
N2a	4120	490	-	-	-	-
N3	3960	479	-	368	-	-
N4	3960	483	-	374	358	366
K1	4330	-	551	388	373	381
K2	4440	-	556	398	401	400
K3	4210	-	580	383	379	381
K4	4150	-	557	379	396	388
C1	3920	396	-	-	-	-
C2	3850	392	-	358	337	348
C3	3900	393	-	363	370	366
C4	3940	398	-	356	371	364
C5	3950	-	546	395	-	-
C6	4000	-	527	385	377	381

TABLE 10-4 TEST RESULTS--TORQUE, ANGLE OF TWIST AND STIFFNESS

Beam	T_{cr}	T_u	Angle of Twist 10^{-3} deg/in.		K_{tcr}
	in.-kips	in.-kips	θ_{cr}	θ_u	10^6 in^2-lb/deg
B1	182	197	2.70	62	-
B2	177	259	2.88	68	2.44
B3	178	332	3.15	75	4.10
B4	194	419	3.02	83	5.76
B5	200	497	3.50	90	6.52
B6	221	546	4.14	95	8.40
B7	179	238	2.75	70	2.46
B8	193	288	3.20	-	3.94
B9	174	264	2.70	74	2.12
B10	156	304	2.25	80	6.60
D1	133	198	2.04	52	2.88
D2	123	245	1.88	58	3.70
D3	134	346	2.07	71	5.80
D4	140	424	2.24	81	7.00
M1	170	269	2.70	64	2.28
M2	182	359	2.81	75	4.44
M3	183	388	3.07	78	4.78
M4	183	439	3.41	84	5.68
M5	192	493	3.08	91	7.56
M6	201	532	3.71	-	7.98
I2	220	319	3.60	65	3.30
I3	226	404	2.70	69	4.64
I4	248	514	3.13	-	6.60
I5	249	626	3.87	78	8.00
I6	244	679	3.24	80	8.84
J1	124	190	2.17	67	1.62
J2	151	258	3.15	75	3.38
J3	150	312	2.44	80	3.92
J4	159	360	2.79	85	4.94
G1	237	237	2.51	-	-
G2	268	357	2.73	72	4.06
G3	240	439	2.44	74	5.24
G4	254	574	2.97	78	6.52
G5	261	637	2.89	79	7.16
G6	274	346	2.76	61	4.00
G7	298	466	3.42	65	6.46
G8	298	650	3.13	72	8.14
N1	67.2	80.5	3.25	110	0.40
N1a	62.2	79.6	2.75	110	0.40
N2	65.9	128	5.52	125	0.85
N2a	66.4	117	5.34	123	0.83
N3	65.6	108	5.41	119	0.67
N4	67.3	139	5.38	130	1.00
K1	109	136	4.00	80	1.19
K2	108	210	4.51	-	1.68
K3	110	252	4.90	110	2.49
K4	116	310	5.23	125	3.36
C1	100	100	3.06	-	-
C2	98	135	3.24	90	0.88
C3	105	177	3.06	-	1.83
C4	105	224	3.42	113	2.17
C5	124	263	4.22	123	3.27
C6	123	303	4.36	133	4.18

longitudinal bars, two on an upper bar and two on a lower bar, at about the third-points of the effective beam length. Six gages were also mounted on three closed stirrups located at the center and about the third-points of the effective length. Each stirrup had one gage at the center of a longer leg and another at the center of a shorter leg. When two additional longitudinal bars were placed at the center of the wider cross-section face, as in some beams of Series G, N, K, and M, one of these two longitudinal bars was gaged. At the same time the gage at the center of the longer leg of each stirrup was moved upward about 1 1/2 in. to avoid interference with these added longitudinal bars. The observed stresses are recorded in Table 10-5. In some beams, additional stresses in the reinforcement were also measured at locations other than those mentioned above.

Strains on the surface of the concrete were measured by Type A-9-4 SR-4 gages of 2 1/2 in. length. They were located at the center of the wider face and orientated at 45 deg to the axis of the beam to obtain the principal compressive or principal tensile stresses. The principal compressive strains immediately before cracking and at ultimate load are also given in Table 10-5. The principal tensile strains, however, were found to be of no significance once cracking occurred; they are not reported. In some beams, the principal strains at the other locations were measured.

All outputs of load cells, Metrisite, and SR-4 gages were fed into Sanborn Type 67A recorders to obtain continuous readings. The cracking torque and ultimate torque may occur while the load is being increased from one increment to the next, and the angles of twist and strains will increase rapidly while the cracking or ultimate torque is being approached. Accurate measurements can therefore be obtained only by continuous recording.

The test beams behaved differently before and after cracking of the concrete. Accordingly, the load increments used were different. About eight load stages were used before cracking, and each load stage required about two minutes to reach a stabilized condition. After cracking, 6 to 12 load increments were used according to the amount of reinforcement in the beams. The load was held constant for 15-20 min after each load application so that the cracks could be traced and crack widths measured. The duration of a complete test was about three hours.

Crack width was measured by a hand microscope with a scale subdivided into 0.001 in. Measurements were taken along the middle 48-in. length of the beams at the center of the wider face. When longitudinal bars were placed at the center of the wider face (such as Beams M6, G6-G8, N3-N4, K1-K4) crack measurement was also made at the quarter-point of the wider face, between two longitudinal bars, because crack width is usually

TABLE 10-5 TEST RESULTS--STRESSES OF REINFORCEMENT AND STRAINS OF CONCRETE

Beam	Tensile Stresses in Reinforcement at T_u						Principal Compressive Strain of Concrete, Millionths	
	Longitudinal Bars		Stirrups Longer Side		Stirrups Shorter Side			
	N[1]	f_s[2]	N[1]	f_s[2]	N[1]	f_s[2]	ϵ_{cr}[3]	ϵ_u
B1	2/6	23.4-27.7	5/6	44.0	0/6	(-3.1)-37.6	-	-
B2	1/3	17.2, 29.5	1/3	27.0, 45.7	-	-	-	-
B3	5/6	46.8	1/3	45.4, 46.0	0/2	(-3.2), 16.5	-	-
B4	2/6	34.1-42.6	1/3	34.8, 41.9	0/3	6.0 -18.2	-	-
B5	2/3	40.9	0/3	27.7-37.6	-	-	-	-
B6	0/6	31.2-48.2	0/3	13.6-33.5	0/3	4.7 -13.5	-	-
B7	6/9	27.1-46.0	0/6	22.8-38.3	0/6	(-10.8)-16.4	260, 265	1135, 2450
B8	6/6	-	0/6	20.5-26.0	0/3	11.4 -16.2	-	-
B9	5/6	35.3	2/3	44.0	0/3	28.4 -47.7	-	-
B10	0/6	24.8-33.5	3/3	-	2/3	42.6	-	-
D1	1/4	30.0-43.5	1/3	24.0, 31.5	1/3	25.4, 29.2	132, 140	803, 1205
D2	1/4	27.5-34.1	0/3	25.3-43.2	0/3	10.8-23.4	127, 99	1330, 1400
D3	1/4	31.2-32.1	2/3	46.2	0/3	21.0-33.4	131, 132	1570, 1585
D4	2/4	42.6, 44.0	0/3	29.8-39.8	0/3	9.1-15.6	133, 144	1888, 2502
M1	1/4	34.8-46.0	2/3	42.8	1/3	22.4, 38.3	212, 174, 196	1980, 1265, 1560
M2	1/8	37.5-48.5	3/3	-	2/3	49.7	227, 236, 213	2480, 3400, 5520
M3	0/4	23.6-35.5	3/3	-	0/3	10.9-22.6	201, 224, 246	2670, 2920, 2270
M4	0/4	19.6-41.5	2/3	42.4	0/3	12.9-23.7	288, 218, 250	3690, 4350, 3070
M5	0/4	27.8-37.2	1/3	41.5, 44.5	0/3	5.0-15.8	242, 256, 238	5290, 4060, 5660
M6	0/4	25.7-35.8	0/3	21.0-33.4	0/3	16.1-18.3	236, 307, 251	-
I2	1/4	36.2-45.4	2/3	35.8	1/3	43.2, 48.2	252, 330	1305, 1880
I3	2/4	27.0, 37.5	2/3	47.1	0/3	14.2-31.4	199, 196	1230, 1470
I4	1/4	29.0-39.5	3/3	-	0/3	20.3-25.0	226, 205	2000, 1815
I5	1/4	39.0-44.0	2/3	38.3	0/3	16.9-27.0	283, 269	2880, 2620
I6	0/4	35.8-42.9	0/3	31.2-37.8	0/3	10.6-22.3	403, 260	3210, 1785
J1	2/4	42.6, 27.0	0/3	31.2-41.2	0/3	16.8-22.7	185, 199	1985, 2410
J2	1/4	29.5-40.6	2/3	41.2	0/3	21.3-35.2	209, 236	2160, 3400
J3	0/4	29.5-44.3	1/3	37.5, 40.6	0/3	11.4-16.1	170, 195	1790, 2265
J4	0/4	29.5-41.1	0/3	19.9-30.9	0/3	8.5-14.3	246, 226	4860, 4320
G1	0/4	.02- .06	0/3	.07-42	0/3	.01- .03	98, 218	-
G2	2/4	22.7, 39.0	2/3	42.9	1/3	34.9, 47.4	274, 198	- , 1320
G3	0/4	19.5-33.8	3/3	-	0/2	(-5.0), 18.5	260, 170	1980, 1275
G4	2/4	33.5, 42.0	3/3	-	0/3	6.6-24.0	200, 250	2200, 1730
G5	0/4	39.3-43.5	0/3	41.5-43.2	0/3	.36-13.5	222, 199	2790, 1615
G6	3/6	30.1-43.4	3/3	-	1/3	33.2, 46.9	255, 274	1030, 2640
G7	8/8	-	2/3	42.6	0/3	14.3-22.7	222, 298	2170, 1490
G8	3/6	31.2-36.9	3/3	-	0/3	11.5-28.4	267, 302	4530, 3520
N1	3/4	46.6	2/3	48.3	0/3	20.2-40.5	260, 368, 227	1240, 2840, 1420
N1a	2/4	43.2, 49.1	1/3	40.3, 43.5	0/3	33.8-47.8	194, 259, 283	1580, 1980, 1930
N2	1/4	42.0-46.1	3/3	-	0/3	19.3-39.2	312, 255, 264	3450, 2700, 2620
N2a	1/4	29.2-43.1	3/3	-	0/3	3.3-34.6	236, 314, 295	5200, 4630, 5200
N3	5/6	45.4	3/3	-	2/3	37.2	286, 354, 354	2900, 3470, 1940
N4	2/5	34.1-45.4	0/3	43.3-45.1	0/3	18.6-39.7	302, 286, 293	5000, 4250, 4110
K1	4/4	-	3/3	-	0/3	1.7-14.6	253, 211	1320, 1490
K2	3/4	36.9	2/3	47.2	0/3	4.9-18.7	226, 275	1780, 2560
K3	2/4	38.9-45.4	1/3	42.5, 44.2	0/3	14.9-19.9	198, 232	2600, 1890
K4	0/4	30.9-45.7	0/3	40.6-45.7	0/3	4.8- 9.9	288, 286	4250, 3090
C1	1/4	(-0.50)-0.65	0/4	(-0.30)-1.40	-	-	142, 189	-
C2	1/4	27.0-38.9	0/4	26.4-42.6	-	-	-	-
C3	0/4	14.6-31.7	0/4	18.3-24.4	-	-	255, 166	1322, 1180
C4	0/4	26.0-43.2	0/4	5.0-20.3	-	-	-	-
C5	0/4	27.3-36.6	0/4	2.8-14.9	-	-	206, 364	2550, 3450
C6	0/4	16.7-28.8	0/4	(-15.6)-12.8	-	-	301, 272	3100, 2620

[1] Fraction of gages yielded. The numerators are number of gages yielded, while the denominators are the number of gages installed.

[2] Tensile stresses measured by the unyielded gages. Negative sign in brackets means compression.

[3] Immediately before cracking.

largest at that location. In some beams, crack measurements were also made along the edge of the wider face and along the center of the shorter face.

Presentation of Results

The behavior of reinforced concrete beams subjected to torsion can be divided into two distinct stages: before and after cracking of the concrete. Before cracking, a beam behaves essentially as a plain concrete beam without reinforcement. The stresses in the reinforcement are small, and the torque-twist curve is almost identical to that of a plain concrete beam.

When cracking of the concrete occurs, the stresses in the reinforcement increase suddenly and the beam twists under constant torque until it reaches a new state of equilibrium. Thereafter, the applied torque can be further increased, but the stiffness of the beam is only a fraction of that before cracking. Consequently, the presentation and analysis of test results are divided into two parts--the behavior before cracking and after cracking. Observed behavior characteristics are given in two appendices: torque-twist curves are given in Appendix A, strain data in Appendix B.*

BEHAVIOR BEFORE CRACKING

General Behavior

It was found that the cracking torque, T_{cr}, of a reinforced concrete beam is 1.0 to 1.3 times the failure torque of its corresponding plain** concrete beam, T_{up}, as computed by Eq. (1). For the range of loading below T_{up}, the stresses in the reinforcement were very small, as shown for Beam G4 in Fig. 10-4. The torsional stiffness and the concrete strains were also very close to those of corresponding plain concrete beams. For example, the slope of the torque-twist curve for Beam G4 at zero torque was $143 \cdot 10^6$ in.^{2}-lb/deg, as compared to 146 and 144 for the corresponding plain Beams A5 and A6 in Reference 2. At the ultimate torque of the plain beams, 216 in.-kips, the angle of twist for

*The Appendices are not included in this volume. The material in the Appendices will be on permanent file at ACI headquarters and will be available at cost of reproduction. For those living in the United States and Canada, a convenient reprint of the paper including the Appendices will be available as a Bulletin of the Development Department, Portland Cement Association.

**A corresponding plain concrete beam means a beam with the same material and dimensions as the reinforced concrete beam, but entirely without reinforcement.

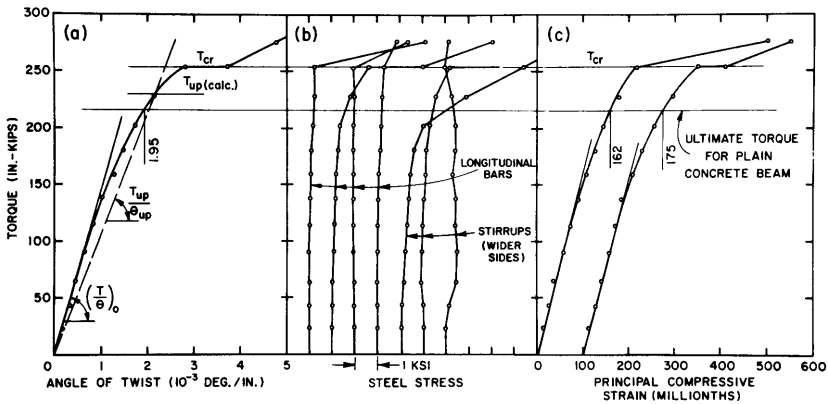

FIG. 10-4 BEHAVIOR OF BEAM G4

G4 was $1.95 \cdot 10^{-3}$ deg/in. as compared to 1.89 and 2.21 for the plain beams. At this same torque, the principal compressive strains were 162 and 175 millionths for G4 as compared to 155 and 160 for A5, and 146 and 171 for A6.

When applied torque exceeded T_{up}, stress began to develop in the reinforcement; concrete stresses and angle of twist increased somewhat more rapidly. Again, the behavior of Beam G4 shown in Fig. 10-4 is typical. Angles of twist immediately before cracking, θ_{cr}, are given for all specimens in Table 10-4; the corresponding principal concrete strains, ε_{cr}, are reported in Table 10-5.

Cracking Torque

When cracking was first seen on the concrete surface and the stresses in the reinforcement increased suddenly, it was considered that the cracking torque, T_{cr}, was reached. Its magnitude was about 1.0-1.3 times the failure torque of the corresponding plain concrete beam, T_{up}. This strengthening is apparently due to the reinforcement, and it should increase with increasing amount of reinforcement. The ratio T_{cr}/T_{up} is plotted in Fig. 10-5 as a function of the total volume percentage of reinforcement, p_t. The straight line shown is expressed by

$$T_{cr} = (1.00 + 0.04\ p_t)\ T_{up} \qquad (3)$$

where

p_t = total volume percentage of reinforcement

T_{up} = failure torque given in Eq. (1) for the corresponding beam without reinforcement

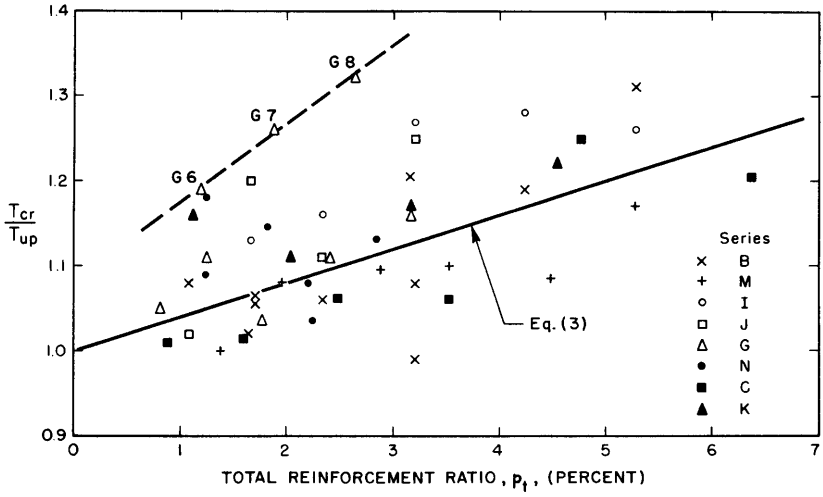

FIG. 10-5 CRACKING TORQUE AS A FUNCTION OF REINFORCEMENT RATIO

A broken line is shown at the upper left of Fig. 10-5 connecting points of Beams G6 to G8. These three beams have six longitudinal bars, with two located at the center of the wider face. Their higher T_{cr}/T_{up} ratio shows that a better distribution of reinforcement will increase the cracking torque somewhat, so that Eq. (3) becomes conservative.

Torsional Stiffness

The torsional stiffness of an elastic rectangular member according to Saint-Venant's theory is

$$K_t = \frac{T}{\theta} = G \beta x^3 y$$

in which

K_t = torsional stiffness

G = modulus of rigidity

β = a coefficient

In the case of concrete members, G is difficult to measure, and it is not a constant because the stress-strain curve of concrete is not linear. A good estimate of the torsional stiffness can be obtained by the ratio

$$K_t = T_{up}/\theta_{up} \qquad (4)$$

in which T_{up} and θ_{up} are given by Eq. (1) and (2), respectively.

An example is given for Beam G4 in Fig. 10-4a. The broken line with a slope of T_{up}/θ_{up} appears to be a good approximation of the torque-twist curve before cracking. Since T_{up} and θ_{up} are failure torque and angle of twist at failure, respectively, of a corresponding plain concrete beam, this slope also has a physical meaning, the secant slope at the failure of the torque-twist curve for a corresponding plain concrete beam.

BEHAVIOR AFTER CRACKING

General Behavior

As described above, a reinforced concrete beam behaves before cracking like a beam without reinforcement; it follows approximately Saint-Venant's elastic torsional theory. However, Saint-Venant's theory was often wrongly applied by many investigators to predict the behavior of reinforced concrete beams after cracking. For example, according to such application of Saint-Venant's theory, the stresses in the longitudinal bars located at the four corners of a rectangular cross-section should be zero, while stresses in bars located at the center of the wider face should be a maximum. The test results show that these stresses were essentially equal regardless of the location of the longitudinal bars. Similarly, the theory predicts that stresses in a closed stirrup should vary from zero at the corners to a maximum at the center of the longer leg. Tests reveal that the stresses were actually uniform along the longer legs of the stirrups. Furthermore, the maximum principal stresses at the center of the wider cross-section face were roughly 3 or 4 times those according to Saint-Venant's theory. In some cases the principal compressive strains exceeded 0.004. It must be concluded, therefore, that Saint-Venant's theory cannot be applied to a reinforced concrete beam after cracking, because cracking terminates Saint-Venant's basic assumption that the material is continuous.

The torque-twist curves of Beams B1-B6 after cracking are shown in Fig. 10-6a. These beams are identical except that the amount of reinforcement increases from B1 to B6. The stresses in the longitudinal and stirrup reinforcement of these beams were plotted against T/T_u, the ratio of torque over ultimate torque, in Fig. 10-6b. This nondimensional ratio was introduced for simplicity of presentation. Fig. 10-6a shows that, upon cracking, the angle of twist increased significantly under a constant torque, and Fig. 10-6b reveals that the stresses in the reinforcement increased suddenly. This behavior indicates that the equilibrium condition that existed in the uncracked reinforced concrete beam was upset by the cracking so that the beam sought a new equilibrium condition by transferring load to the reinforcement. At the end of this twisting under constant torque, a new equilibrium condition

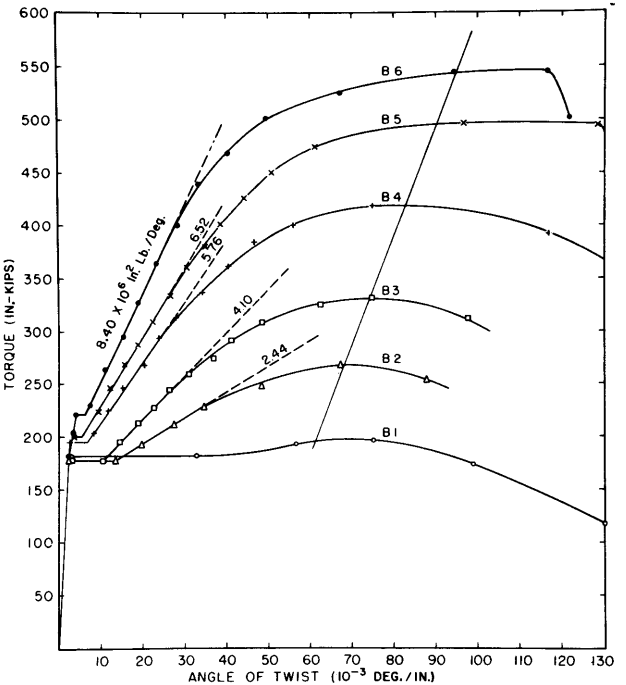

FIG. 10-6a TORQUE-TWIST CURVES OF BEAMS B1-B6

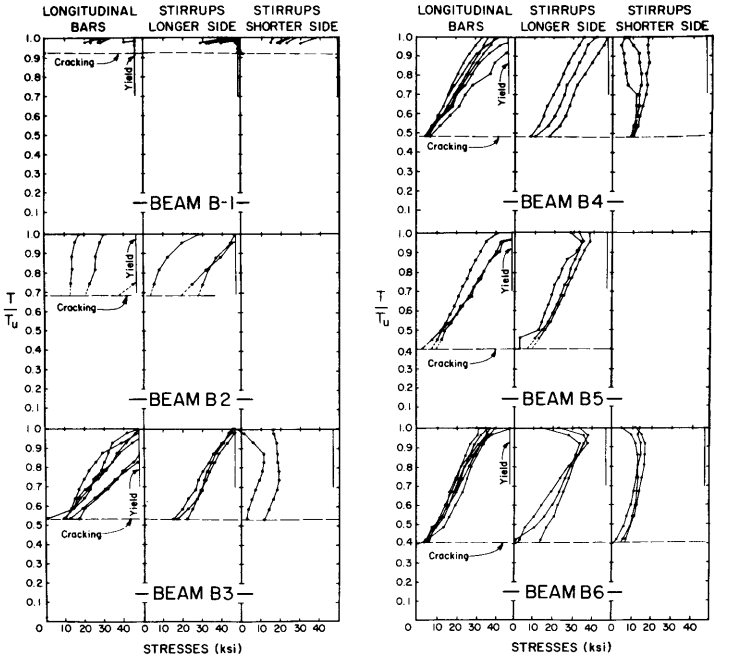

FIG. 10-6b STEEL STRESSES OF BEAMS B1-B6

was established, and the tensile stresses in the reinforcement stabilized. In the case of Beam B1, which had a very small amount of reinforcement, the angle of twist under constant torque after cracking was very large, and the stresses in the reinforcement increased almost to the yield point. However, as the curves for the other beams show, the angle of twist and steel stresses immediately after cracking decrease with increasing amount of reinforcement.

The principal compressive strains were not measured in this Series B, but their characteristics can be observed from Series G. The torque-twist curves, the stresses in the reinforcement, and the principal compressive strains are given for Series G in Fig. 10-7a and 10-7b. Torque-twist curves for other series can be found in Appendix A, the steel stresses and concrete strains in Appendix B. Fig. 10-7b shows that the principal compressive strain also increased suddenly upon cracking. The additional strain can be as much as three times the strain before cracking, but it decreases with increasing amount of reinforcement and becomes rather small for large amounts of reinforcement.

This behavior of increasing angle of twist under a constant torque upon cracking is significant when compared with the moment-rotation curve of a flexural beam. When cracking occurs in a flexural beam, the slope of the moment-rotation curve

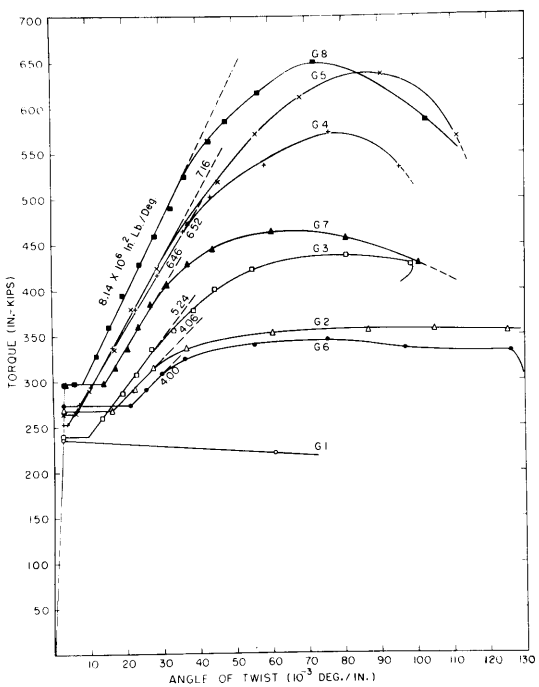

FIG. 10-7a TORQUE-TWIST CURVES OF BEAMS G1 - G8

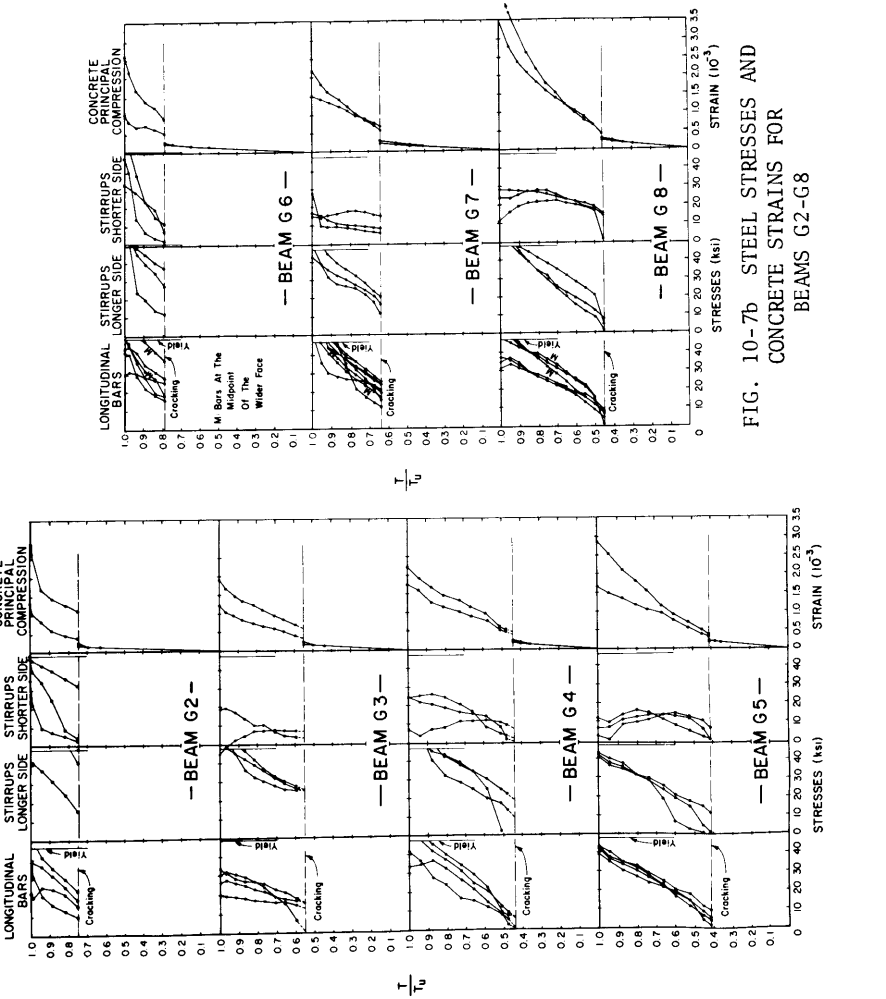

FIG. 10-7b STEEL STRESSES AND CONCRETE STRAINS FOR BEAMS G2-G8

suddenly decreases and the curve begins to follow a new slope. However, there is no increasing rotation under a constant bending moment. This difference may be due to the mechanisms of equilibrium before and after cracking. When cracking occurs in flexural beams, the tensile stresses resisted by the concrete before cracking are simply transferred to the reinforcement. There is no major change in the mechanism of equilibrium, and there should not be any abrupt change of behavior. On the other hand, cracking of a torsion beam under torque changes the Saint-Venant type of equilibrium into a new type. Since the conditions of equilibrium before and after cracking are different, a transitional behavior of twisting under constant torque should occur. This new type of equilibrium after cracking is proposed to be an equilibrium of moments and forces on a failure plane perpendicular to the wider face and inclined at 45 deg to the axis of the beam. It will be carefully treated in a later paper with development of a new ultimate torsional strength theory.

The torque-twist curves in Fig. 10-6a show that, when a beam stabilized after cracking, the curve began to rise again. It was first essentially a straight line, then curved toward the horizontal when the ultimate strength was approached. The slope of the straight portion, which is the torsional stiffness after cracking, was only a fraction of that before cracking. It increased with increasing amount of reinforcement from Beam B1 to B6. At the same time the stresses in the steel and the principal compressive strain of concrete at the center of the wider face increase approximately linearly with loading as shown in Fig. 10-6b and 10-7b, except for the stresses in the shorter legs of the stirrups. The latter increased at first and then acted irregularly, often decreasing when the ultimate strength was approached. In some cases these stirrup stresses became compressive at the ultimate torque, such as one gage in Beams B1 and B3 of Fig. 10-6b and one gage in Beam G3 of Fig. 10-7b. This peculiarity is worth emphasis because it cannot be explained by present theories.

The ultimate torque of a beam depends to a large extent on the amount of reinforcement, as shown in Fig. 10-6a. At the ultimate torque Fig. 10-6b shows that the stresses in the longitudinal bars and in the longer legs of the stirrups can both reach the yield point when small percentages of reinforcement are used, such as for Beams B1 to B3. However, they cannot reach yielding with a large percentage of reinforcement, such as Beam B6. This means that Beam B6 was over-reinforced. For Beams B4 and B5, the longitudinal bars yielded, but the stirrups did not. This indicates that these beams were over-reinforced in stirrups only. In Beams B1-B6 the ratio, m (volume of longitudinal bars to volume of stirrups), was unity. This ratio was too low. In other words, the balanced ratio, m_b, which will guarantee that both

longitudinal bars and stirrups reach yielding, is not necessarily unity as assumed in the existing theory of torsion for reinforced concrete members.[3,4] This is discussed later.

The principal compressive strain at the ultimate torque also increased with increasing percentage of reinforcement as shown in Fig. 10-7b. When a beam is over-reinforced, this strain can exceed 0.004, which is well over the peak of the stress-strain curve of concrete and into the descending branch.

Considering both steel stresses and the concrete strain, it can be concluded that reinforced concrete beams subject to torsion can be divided into three types: (1) under-reinforced beams in which yielding of all steel causes failure; (2) completely over-reinforced beams in which the steel does not yield, so that failure is due to primary crushing of the concrete; and (3) partially over-reinforced beams in which either the longitudinal bars or stirrups yield at failure but the concrete crushes before the other steel yields. Spalling of concrete can always be observed at failure somewhere at the wider face of the beam, even for under-reinforced beams. This is similar to under-reinforced flexural beams in which the yielding of the tension steel causes the maximum concrete strain at the outer fiber to increase rapidly so that spalling occurs during final failure of the beam. In the pure torsion tests, spalling was never observed on the shorter face of a beam; crushing of the concrete took place only on the wider face of the beam.

Beyond the ultimate torque, Fig. 10-6a and 10-7a show that the torque-twist curves exhibited a definite descending branch. However, these descending branches were obtained in a matter of seconds. They may also terminate abruptly, possibly due to release of the energy stored in the torsion test rig. A change of testing methods from constant rate of loading to constant rate of twist might change this behavior. In any case, it appeared that in general the descending branches of the torque-twist curves for under-reinforced beams were longer than those for over-reinforced beams, which terminated shortly beyond maximum torque.

Ultimate Torque

Ultimate torque is defined as the maximum torque which can be resisted by the member. According to Section 2.22 of the 1958 German Code[5] and Section 615 of the 1958 Australian Code,[6] the equation for ultimate torque is

$$T_u = T_o + \Omega\, x_1 y_1 \frac{A_s f_{sy}}{s} \tag{5}$$

where

T_u = ultimate torque

T_o = (in the Australian Code) the failure torque of the beam without reinforcement according to Saint-Venant's theory

T_o = zero in the German Code

Ω = a constant, 2 and 1.6 for the German and Australian codes, respectively

x_1 = smaller center-to-center dimension of a closed rectangular stirrup

y_1 = larger center-to-center dimension of a closed rectangular stirrup

A_s = cross-sectional area of one stirrup leg

f_{sy} = yield strength of stirrups

s = spacing of stirrups

The parameter $x_1 y_1 (A_s f_{sy}/s)$ can be used to advantage in analysis of test results. The effect of each variable on the ultimate torque will be treated separately.

Amount of Reinforcement - The ultimate torque of beams in Series B is plotted against the parameter $x_1 y_1 (A_s f_{sy}/s)$ in Fig. 10-8. It can be seen that the relationship is a straight line through points B1 to B3, then turns gradually toward the horizontal. The whole curve can be approximately divided into three straight segments as shown by the dotted lines. The first straight line through points B1 to B3 corresponds to under-reinforced beams, where both the longitudinal bars and the longer legs of the stirrups yielded before the ultimate torque was reached. The second straight portion through points B4 and B5 corresponds to partially over-reinforced beams in which the stirrups did not yield. The last horizontal line through point B6 corresponds to completely over-reinforced beams, where neither longitudinal bars nor stirrups yielded so that the beam failed by primary crushing of the concrete.

For under-reinforced beams, the parameter $A_s f_{sy}/s$ appears to be acceptable. The slope, Ω, of the first straight portion was 1.20, and the ultimate torque can be expressed by

$$T_u = T_o + 1.20\, x_1 y_1 \frac{A_s f_{sy}}{s} \tag{6}$$

where

T_o = the torque for the intercept of the ordinate, 75 in.-kips

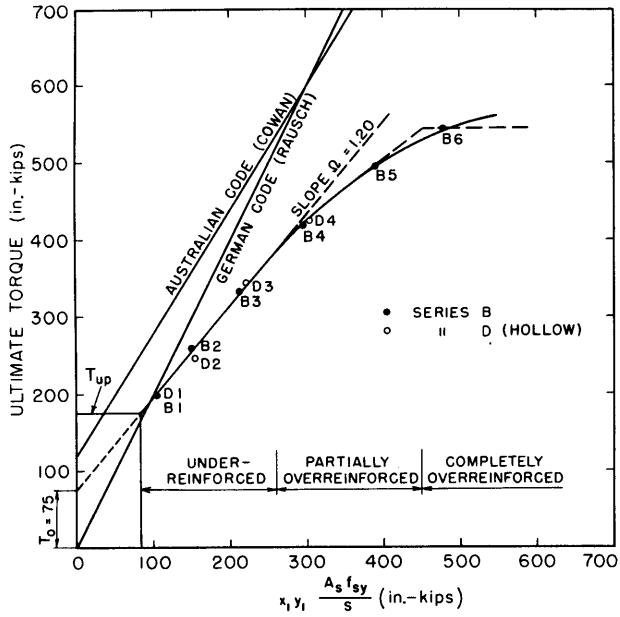

FIG. 10-8 ULTIMATE TORQUE FOR PARAMETER $x_1 y_1 \frac{A_s f_{sy}}{s}$, SERIES B AND D

The predictions of the German and Australian codes are also plotted in Fig. 10-8. It can be seen that the observed T_o is smaller than that predicted by the Australian Code, but larger than that of the German Code. T_o is commonly thought to be the torsional resistance of the concrete core. Also, the slope of the curve for under-reinforced beams is much smaller than 2 and 1.6 as predicted by the German and Australian codes, respectively. Fig. 10-8 thus indicates that the German and Australian codes may overestimate the ultimate torque.

Lessig's theory,[7] which is the basis of the Soviet Code,[8] is also checked for the case of pure torsion in Fig. 10-9. It can be seen that this theory also overestimates the ultimate torque. In fact, for Series B it is very close to the German Code.

Solid and Hollow Beams - Points for hollow Beams D1-D4 are also shown in Fig. 10-8 and 10-9. In these hollow beams, the reinforcement duplicated that provided in the solid beams of Series B. The only departure from Series B was the absence of the concrete core. The points for both series fall on the same curve; equal amounts of reinforcement led to equal ultimate strength in torsion. It appears, therefore, that the concrete core did not contribute to the ultimate torsional strength of a solid

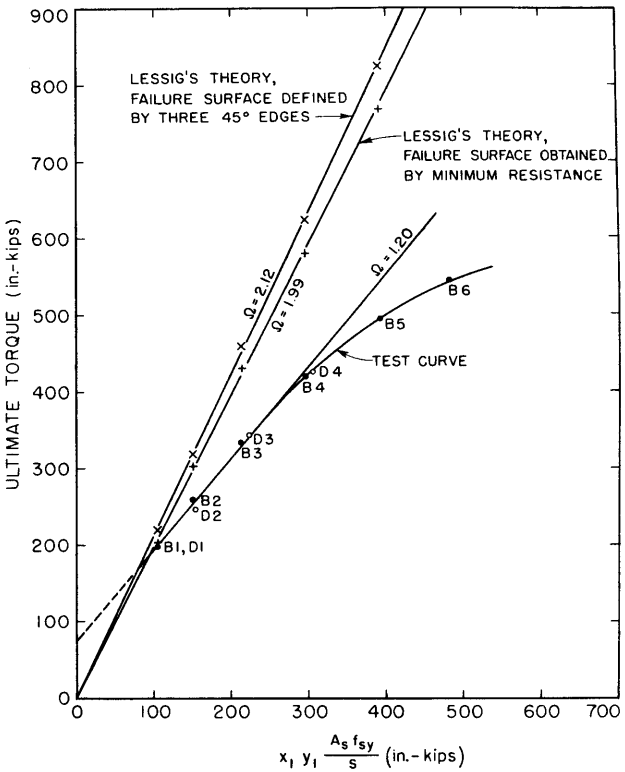

FIG. 10-9 COMPARISON OF LESSIG'S THEORY WITH TEST RESULTS

beam, and the torque T_o was not due to the resistance of the concrete core as is commonly thought. The value of T_o will be examined in detail later in the analysis of the effect of section height/width ratio.

Ratio of Longitudinal Bars to Stirrups - For a reinforced concrete beam subjected to pure flexure, the balanced reinforcement ratio, p_b, produces such beam behavior that the tension reinforcement reaches its yield strength, f_y, just as the concrete in compression fails by crushing. For ratios below p_b, the ultimate moment will be governed by yielding of the steel; for ratios above p_b, primary crushing of the concrete will govern. The balanced ratio, p_b, can be computed as a function of concrete strength, f'_c, and steel yield point, f_y, by well understood flexural theories.

When a reinforced concrete beam is subjected to torsion, the concept of balanced conditions becomes more complex. First, there is a balanced total ratio of longitudinal plus stirrup reinforcement, p_{tb}. When this ratio, p_{tb}, is exceeded, the ultimate

torque will be governed by crushing of the concrete. However, if all reinforcement is to yield under balanced conditions, the total reinforcement, p_{tb}, must be distributed between longitudinal and stirrup reinforcement in a certain ratio, m_b. If the ratio m is greater than m_b, the stirrups will yield, but the longitudinal bars will not. If m is less than m_b, only the longitudinal bars will yield. It appears that p_{tb}, m_b, f'_c and f_y are interrelated in a manner that can only partly be appreciated in the light of available test data.

The ratio, m, for a reinforced concrete beam may be computed by the relationship

$$m = \frac{\bar{A}_\ell \cdot s}{A_s (x_1 + y_1)} \tag{7}$$

where

$\bar{A}_\ell$ = one-half of the total cross-sectional area of longitudinal bars

A_s = area of one stirrup leg

According to the German and Australian codes, m should be taken as unity in all cases. However, it was mentioned above that Beams B4 and B5 of Series B were partially over-reinforced with stirrups, so that the balanced ratio, m_b, for these beams should be greater than unity. To explore m_b further, Beams M1-M6 were tested with m = 1.5, keeping all other variables the same as in Series B. As shown in Fig. 10-10, it was found that Beams M1 and M2 were under-reinforced while Beam M6 was over-reinforced. However, Beams M3-M5 were over-reinforced with longitudinal bars, rather than with stirrups as in Series B. This means that m_b in this case should be less than 1.5. Thus, beams with $y/x = 1.5$, $f'_c = 4000$ psi and $f_{sy} = 48,500$ psi, such as those in Series B and M, should have a balanced ratio m_b between 1.0 and 1.5, probably about 1.2.

The results for Beams B1-B3 and M1-M2 show that, when the total reinforcement is less than about 2.3 percent, m can vary between 1.0 and 1.5 and both longitudinal bars and stirrups will nevertheless yield. As outlined in Table 10-2, a wide range of m from 0.205 to 4.97 was represented by Beams B7 to B10. As expected, Beams B7 and B8 with m of 0.456 and 0.205, respectively, were over-reinforced in stirrups, while Beam B10 with m of 4.97 was over-reinforced in longitudinal bars. However, Beam B9 with $p_t = 1.71$ percent was under-reinforced in spite of the high m-ratio of 2.18. By comparison, Beam B2 has m = 1 and $p_t = 1.65$ percent, and the ultimate strengths of B9 and B2 are 264 in.-kips and 259 in.-kips, respectively. This comparison shows that these two beams with essentially the same p_t have

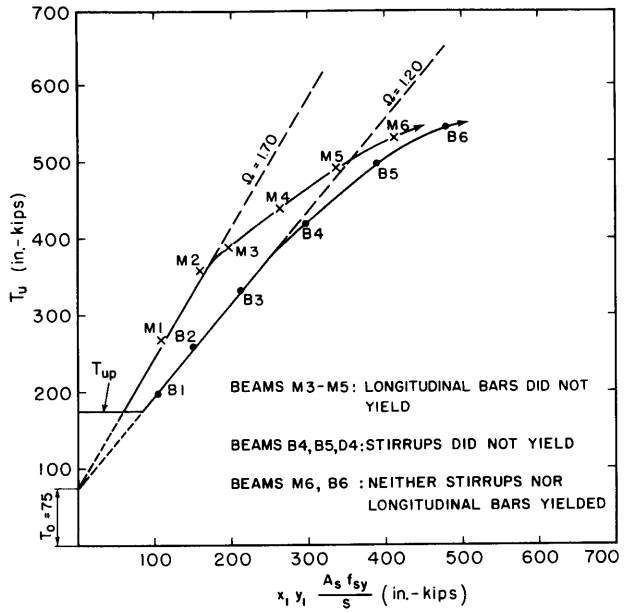

FIG. 10-10 COMPARISON OF SERIES B AND M, WITH m AS VARIABLE

about the same ultimate strength in spite of the large difference in m from 2.18 to 1.0. This is reasonable because both beams are under-reinforced so that all reinforcement was fully utilized.

Although the fully effective value of the ratio m can vary widely for beams with a small percentage of reinforcement, it becomes very sensitive for beams with high percentages of reinforcement, such as Beams B4-B5 and M3-M5. Further research regarding this ratio is needed to assure full utilization of reinforcement.

The German and Australian codes imply that, in the case of m = 1.5 as in Series M, the additional longitudinal bars in excess of m = 1.0 should not contribute to the ultimate torque. On the contrary, Fig. 10-10 shows that these additional longitudinal bars can contribute significantly to the ultimate strength. It is also interesting to note that the torque T_o for Series M is equal to that of Series B; T_o seems to be independent of m.

Concrete Strength - In Series B the average concrete cylinder strength, f'_c, was 4170 psi. In order to study the influence of f'_c on the ultimate torque, Series I and J were tested with average concrete strengths of 6550 and 2270 psi, respectively, while keeping all the other variables the same as in Series B. The results are plotted in Fig. 10-11 together with those of Series B. Beams I2-I5 and J1-J2 were under-reinforced. By drawing straight

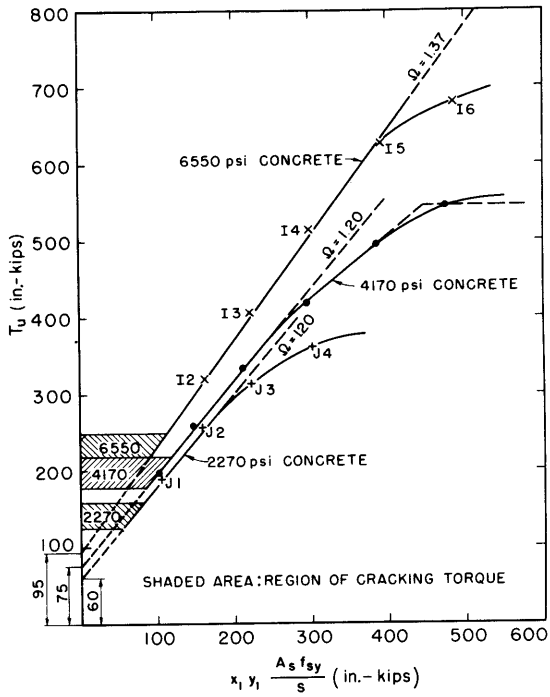

FIG. 10-11 COMPARISON OF SERIES I, B AND J, WITH CONCRETE STRENGTH AS VARIABLE

lines through the points of these beams, T_o was obtained as 95, 75 and 60 in.-kips for Series I, B, and J, respectively. By plotting T_o versus f'_c in Fig. 10-12, it was found that T_o is approximately a function of $\sqrt{f'_c}$. Similarly, Ω was obtained as 1.37, 1.20, and 1.20 for Series I, B, and J, respectively.

Fig. 10-11 also shows that, for m = 1.0, the balanced total percentage of reinforcement, p_{tb}, defined as the maximum p_t which will ensure yielding of both longitudinal bars and stirrups at maximum torque, increases with increasing concrete strength. Furthermore, the ratio of m = 1 used for Series I is very close to the balanced ratio, m_b, because both longitudinal bars and stirrups yielded in Beam I5, while neither yielded in Beam I6. As discussed previously, this is not the case for Series B where Beams B4 and B5 were over-reinforced in stirrups, and it was determined that m_b should be about 1.2. Thus, m_b decreases with increasing f'_c.

Scale Effects - A rectangular cross-section can be defined by two variables: the height-to-width ratio, and an absolute dimension, either the height, width, or cross-sectional area. The latter variable is called size effect or scale effect.

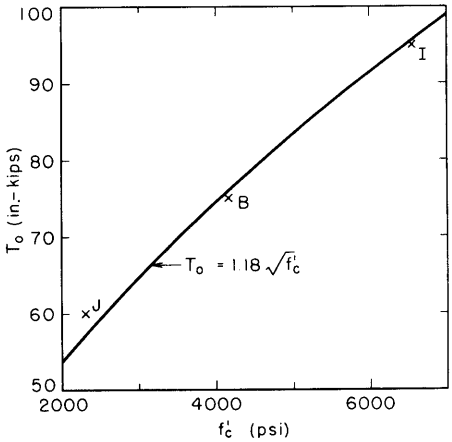

FIG. 10-12 T_o AS A FUNCTION OF f'_c

In the German and Australian codes, T_u is accepted as a linear function of $x_1 y_1$. In other words, Ω is a constant and not a function of size of specimen. In order to check this law of similitude, Series G and N were tested with equal height-to-width ratio so that the scale effect was isolated. The beams in Series G had a cross-section of 10 x 20 in. while those in Series N were 6 x 12 in. The latter were exact 3/5-scale replicas of the former in all aspects.

The ultimate torque is plotted for Series G and N in Fig. 10-13a and 10-13b, respectively. It was found that Ω was 1.45 for Series G and 1.30 for Series N, which indicated that the law of similitude does not hold. This phenomenon needs further research because it is important in model testing, in which the ultimate torque of a model is usually assumed to be linearly related to that of its prototype.

Height-to-Width Ratio of Section - Since the law of similitude is in question, the effect of height-to-width ratio must also be studied by keeping one dimension of the cross-section constant--in this investigation the width, x.

The effect of height-to-width ratio was studied by comparing Series G, B, and C with cross-sections of 10 x 20, 10 x 15 and 10 x 10 in., respectively, while maintaining all the other variables constant. In order to extend the height-to-width ratio in excess of 2, Series N and K were tested with cross-sections of 6 x 12 and 6 x 19.5 in., respectively. The torque T_o and the value of Ω were obtained from Fig. 10-13a and 10-13b and are given in Table 10-6.

Examination of Table 10-6 reveals that T_o is approximately linearly related to $x^{1.5}$ and to y. By plotting T_o versus the

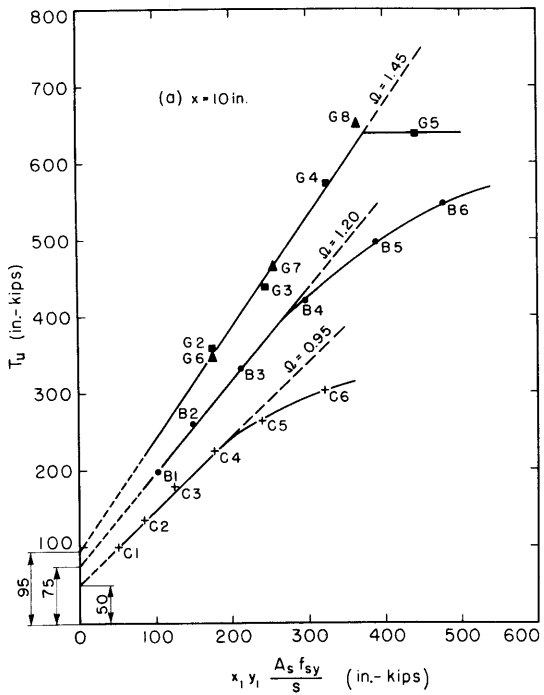

FIG. 10-13a COMPARISON OF SERIES G, B, AND C, WITH CROSS-SECTION AS VARIABLE

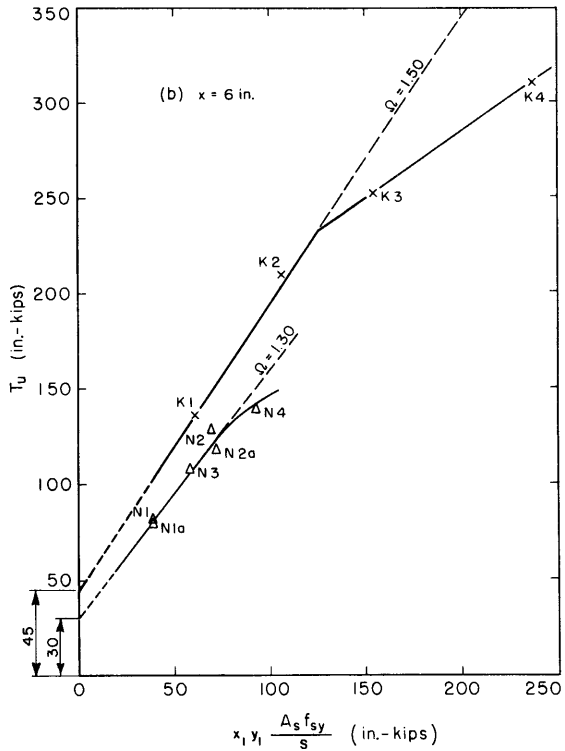

FIG. 10-13b COMPARISON OF SERIES K AND N, WITH CROSS-SECTION AS VARIABLE

TABLE 10-6 T_o AND Ω AS FUNCTIONS OF CROSS-SECTIONAL PROPERTIES

Series of Beams	Cross-Sectional Properties							Test Values		Adjusted Ω		
	x in.	y in.	xy in^2	$x^{1.5}y$	x_1 in.	y_1 in.	y_1/x_1	T_o in.-kips	Ω	x = 10 in. [1]	y = 15 in. [2]	xy = 150 in^2 [3]
1	2	3	4	5	6	7	8	9	10	11	12	13
C	10	10	100	316	8.5	8.5	1.0	50	0.95	0.95	1.02	0.99
B	10	15	150	474	8.5	13.5	1.59	75	1.20	1.20	1.20	1.20
G	10	20	200	632	8.5	18.5	2.18	95	1.45	1.45	1.35	1.38
N	6	12	72	177	5.12	11.12	2.18	30	1.30	1.45	1.35	1.38
K	6	19.5	117	287	4.5	18	4.00	45	1.50	1.67	1.42	1.55

[1] Assuming Ω is a function of x only and using x = 10 in. as basis.

[2] Assuming Ω is a function of y only and using y = 15 in. as basis.

[3] Assuming Ω is a function of xy only and using xy = 150 in^2 as basis.

product $x^{1.5}y$ in Fig. 10-14, it was found that T_o is approximately a linear function of $x^{1.5}y$. Combining the effect of $x^{1.5}y$ (Fig. 10-14) and that of $\sqrt{f'_c}$ (Fig. 10-12), T_o can be written as

$$T_o = C\, x^{1.5}\, y\sqrt{f'_c}$$

where the constant C can be obtained from tests by

$$C = \frac{T_{o,\,test}}{x^{1.5}\, y\sqrt{f'_c}}$$

Fig. 10-15 shows that C can be taken as approximately 2.4, so that

$$T_o = \frac{2.4}{\sqrt{x}}\, x^2 y\sqrt{f'_c}$$

in which x and y are in inches, f'_c in psi, and T_o in in.-lb. In Eq. (8) $1/\sqrt{x}$ appears to represent the scale effect for T_o in the test range, 6 in. < x < 10 in., but is believed to be conservative for x > 10 in.

Table 10-6 also reveals that Ω increases with increasing height-to-width ratio. However, this effect cannot be studied by a direct comparison of the five series of Beams G, B, D, N, and K because the effect of height-to-width ratio is intermixed with the scale effect. To separate these two effects, it was first assumed that Ω is a linear function of the scale effect. However, it is not known whether the scale effect was caused by the width, height, or area of cross-section. Hence, they will be examined separately:

(a) Assuming that the scale effect found in the comparison of Series G and N is caused solely by the width x, Ω can be plotted as a function of x as in Fig. 10-16a where Ω is 1.45 and 1.30 for x of 10 in. (Series G) and 6 in. (Series N), respectively. Using

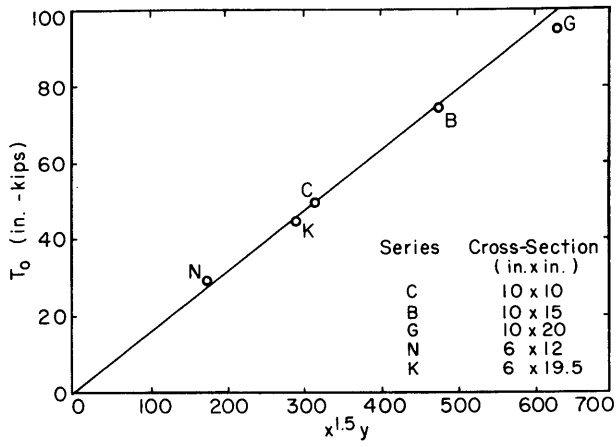

FIG. 10-14 T_o AS A LINEAR FUNCTION OF $x^{1.5}y$

x = 10 in. as a basis of comparison, the coefficient for scale effect will be unity for this point. The coefficient for x = 6 in. is 1.30/1.45 = 0.90. Therefore, the value of Ω for Series N and K, which have 6-in. width, should be divided by 0.90. The adjusted values of Ω using x = 10 in. as a basis are recorded in Column 11 of Table 10-6.

(b) Assuming that the scale effect is caused solely by the height y, Ω can be plotted as a function of y as in Fig. 10-16b. Taking y = 15 in. as a basis of comparison, the coefficient for scale effect should be 1.07, 1.00, 0.96 and 0.93 for y of 20, 15, 12 and 10 in., respectively. Applying these coefficients to Ω, the adjusted Ω using y = 15 in. as a basis are recorded in Column 12 of Table 10-6.

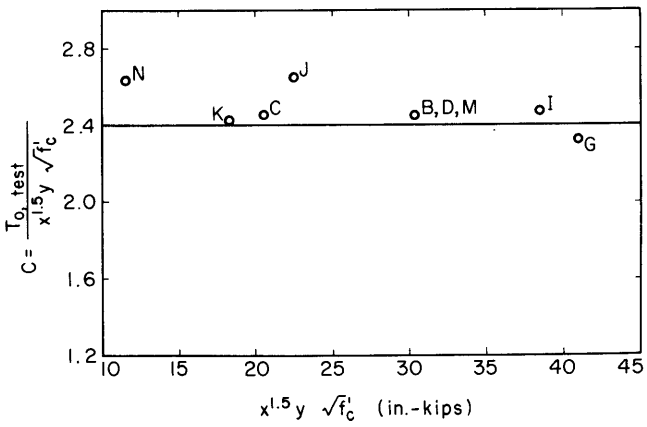

FIG. 10-15 DETERMINATION OF C

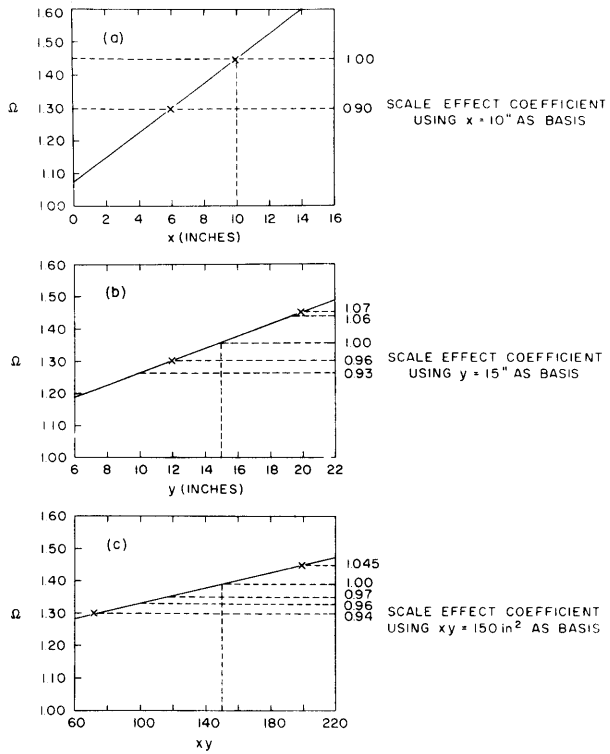

FIG. 10-16 DETERMINATION OF SCALE-EFFECT COEFFICIENT

(c) Assuming that the scale effect is caused by the cross-sectional area, Ω is plotted against xy in Fig. 10-16c. By taking xy = 150 in.^{2} as a basis of comparison, the coefficient for scale effect should be 1.045, 1.00, 0.97, 0.96, and 0.94 for Series G, B, K, C, and N, respectively. The adjusted values are recorded in Column 13 of Table 10-6.

All of the adjusted values of Ω are plotted against y_1/x_1 in Fig. 10-17. It shows that Ω varies linearly at a low range of y_1/x_1 and can be expressed as follows:

Taking x = 10 in. as the basis, and for $y_1/x_1 < 2.7$,

$$\Omega = 0.55 + 0.40\ y_1/x_1 \tag{9a}$$

Keeping y = 15 in., and for $y_1/x_1 < 2.4$,

$$\Omega = 0.75 + 0.28\ y_1/x_1 \tag{9b}$$

Maintaining xy = 150 in^2, for $y_1/x_1 < 2.6$,

$$\Omega = 0.66 + 0.33\, y_1/x_1 \tag{9c}$$

For practical purposes, Eq. (9c) was conveniently used.

It must also be pointed out that the balanced ratio, m_b, is about unity for Series G with y/x = 2.0 as compared with 1.2 for Series B with y/x = 1.5. Thus, m_b appears to decrease with increasing y/x. Hence, the concept of balanced conditions involves not only the aforementioned four variables, m_b, p_{tb}, f'_c and f_{sy}, but also includes y/x.

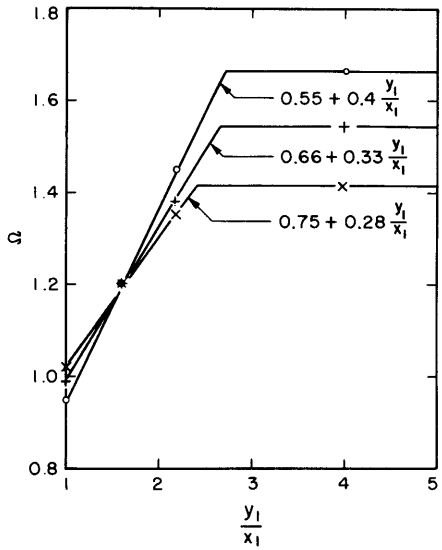

FIG. 10-17 Ω AS A FUNCTION OF y_1/x_1

Spacing of Longitudinal Bars and Stirrups - The effect on the ultimate torque of the spacing of longitudinal bars can be observed most readily in Series G. Beams G2-G5 have four corner longitudinal bars only, while Beams G6-G8 have six longitudinal bars, including the two additional bars located at the center of the longer face. This is to say that the spacing of the longitudinal bars for the latter beams was reduced by one-half. However, Fig. 10-13a shows that the ultimate strengths of Beams G6-G8 fall on the same curve as those of Beams G2-G5. In other words, the spacing of longitudinal bars does not affect the ultimate strength of torsional beams.

The effect of the spacing of stirrups can best be shown by a comparison of Beams N2 and N2a. These two beams were identical in all aspects except that N2 was reinforced with No. 2 stirrups

and 2-in. spacing while N2a has No. 3 stirrups with 4 1/2-in. spacing. The volume percentage of stirrups for these two beams was also identical. Tests showed that Beams N2 and N2a have ultimate strength of 128 in.-kips and 117 in.-kips, respectively. The difference is 9 percent. For practical purposes, this effect of spacing of stirrups will be neglected. This conclusion was also substantiated by examining each series of beams in Fig. 10-10, 10-11, 10-13a and 10-13b because the variation of stirrup spacing within each series of beams did not cause the ultimate strength to deviate significantly from the curves. However, to assure that the ultimate torque will not be lowered significantly by excessively large spacing of stirrups, it is proposed to limit the maximum stirrup spacing to

$$s_{max} = 0.5\ y_1 \tag{10}$$

The physical meaning of this equation is to assure that every 45-deg crack on the wider face of the beam should be crossed by at least two stirrups.

Angle of Twist at Ultimate Torque

Angle of twist at ultimate torque, θ_u, was difficult to determine because it increased very rapidly as ultimate torque was approached. However, Fig. 10-6a showed that θ_u increased with increasing total percentage of reinforcement, p_t. The values of θ_u in Table 10-4 were thus obtained by drawing a straight line through the peaks of all of the torque-twist curves of Beams B1-B6.

Examination of θ_u in Table 10-4 and in torque-twist curves such as Fig. 10-6a shows that θ_u is mainly a function of three variables, namely, the width of the cross-section, x, the height-to-width ratio, y/x, and the total percentage of reinforcement, p_t. All the other variables investigated--the ratio of volume of longitudinal bars to volume of stirrups, m, the concrete strength, f'_c, and the spacing of longitudinal bars and stirrups--have only small influence on θ_u. They were not taken into account in the following analysis.

Studying the cross-section variables, x and y/x, it was found that θ_u has essentially the same parameter

$$\frac{1}{\beta x}\left(1 + \frac{10}{x^2}\right)$$

as θ_{up} for plain members as given by Eq. (2). Expressing θ_u as a function of θ_{up} and p_t, as in Fig. 10-18, leads to the following equations:

$$\theta_u = (28 + 3.2\ p_t)\,\theta_{up} \tag{11}$$

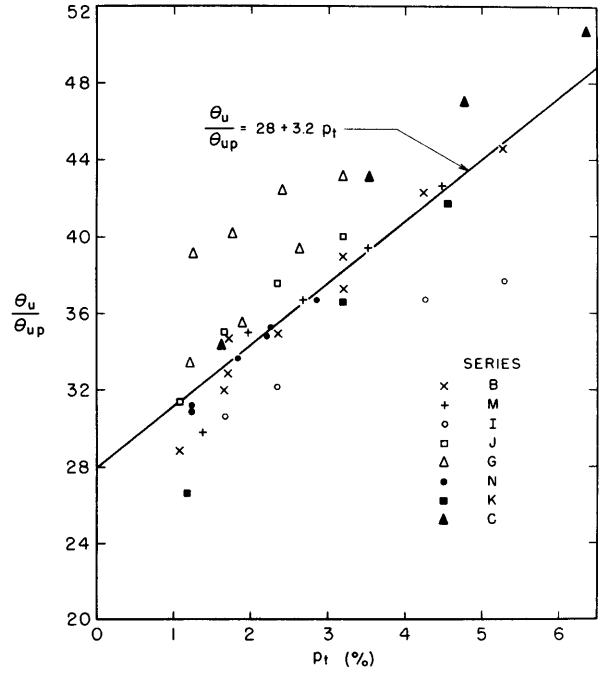

FIG. 10-18 θ_u/θ_{up} AS A FUNCTION OF p_t

or

$$\theta_u = \frac{0.106 + 0.012\ p_t}{\beta\ x}\left(1 + \frac{10}{x^2}\right) \qquad (11a)$$

where θ_u is expressed in deg/in., p_t in percent, and x in inches.

Torsional Stiffness After Cracking

As in the case of θ_u, the torsional stiffness of reinforced concrete rectangular beams shortly after cracking, K_{tcr}, was also found to be mainly a function of x, y/x, and p_t. By plotting T/T_{up} versus θ/θ_{up}, it was found that the initial slope of the curves after cracking, S, is a function of p_t alone. This slope was plotted against p_t in Fig. 10-19 for all test series except the hollow beams of Series D. It can be expressed by

$$S = \frac{T/T_{up}}{\theta/\theta_{up}} = 0.021\ p_t \qquad (12)$$

where p_t is given in percent. Thus, the torsional stiffness after cracking is

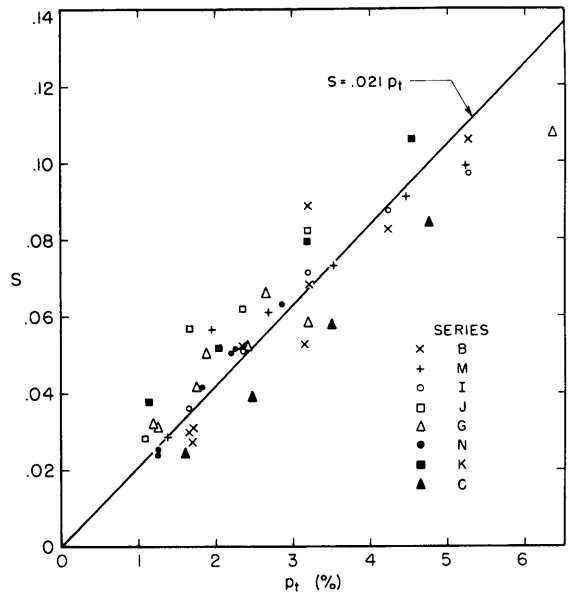

FIG. 10-19 S AS A FUNCTION OF p_t

$$K_{tcr} = \frac{T}{\theta} = S \frac{T_{up}}{\theta_{up}} = 0.021\, p_t \frac{T_{up}}{\theta_{up}}$$

where T_{up} and θ_{up} are given in Eq. (1) and (2).

Since T_{up}/θ_{up} is the torsional stiffness before cracking, K_t, given by Eq. (4),

$$K_{tcr} = 0.021\, p_t K_t \qquad (13)$$

Thus, the beam is much stiffer before cracking than after. Eq. (13) states that the torsional stiffness shortly after cracking is only ($0.021\, p_t$) times the torsional stiffness before cracking.

Angle of Twist at Cracking Torque

It has been shown that upon cracking a beam twists under a constant torque. The torque-twist curve is made up of three distinct regions as shown graphically by the solid curve in Fig. 10-20. Region (a) is the curve before cracking, the slope of which can be approximated by $K_t = T_{up}/\theta_{up}$ as shown in Eq. (4); region (b) is the horizontal plateau and can be calculated by $T_{cr} = T_{up}$ $(1 + 0.04\, p_t)$ from Eq. (3); and region (c) is the curve after cracking, the slope of which can be approximated by $K_{tcr} = 0.021 K_t$

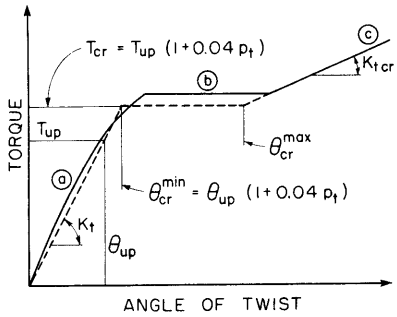

FIG. 10-20 GRAPHICAL DEFINITIONS OF θ_{cr}^{min} AND θ_{cr}^{max}

from Eq. (13). Based on Eq. (4) and (3), two dotted lines can be drawn in Fig. 10-20 to approximate regions (a) and (b), respectively, of the experimental torque-twist curve. The intersection of these two dotted lines gives a theoretical minimum value of the angle of twist at cracking torque:

$$\theta_{cr}^{min} = \theta_{up}\ (1 + 0.04\ p_t) \tag{14}$$

In order to locate region (c) it is necessary to know θ_{cr}^{max}, the maximum angle of twist at cracking torque. Observation of the torque-twist curves such as Fig. 10-6a and 10-7a clearly shows that θ_{cr}^{max} is a function of the amount of reinforcement. By plotting $\theta_{cr}^{max}/\theta_{cr}^{min}$ versus p_t for all beams in Fig. 10-21 (except Series D and Beams B8 and B10 which have extreme values of m), an empirical equation was established for an estimation of θ_{cr}^{max}.

$$\theta_{cr}^{max} = \frac{p_t + 1.5}{p_t - 1}\ \theta_{cr}^{min} \tag{15}$$

where p_t is in percent and must be larger than unity.

Crack Pattern, Width, and Spacing

Diagonal cracks occurred on the wider and shorter faces almost simultaneously. With increasing torque, additional cracks occurred and some of the cracks on the wider faces turned into the shorter faces with a direction almost perpendicular to the longitudinal axis of the beam. These cracks combined with the existing 45-deg cracks at the shorter faces so that some cracks on the shorter faces looked like S-shaped curves. Of course, some of the 45-deg cracks on the shorter faces also turned perpendicularly into the longer face, but they appeared to have no significance.

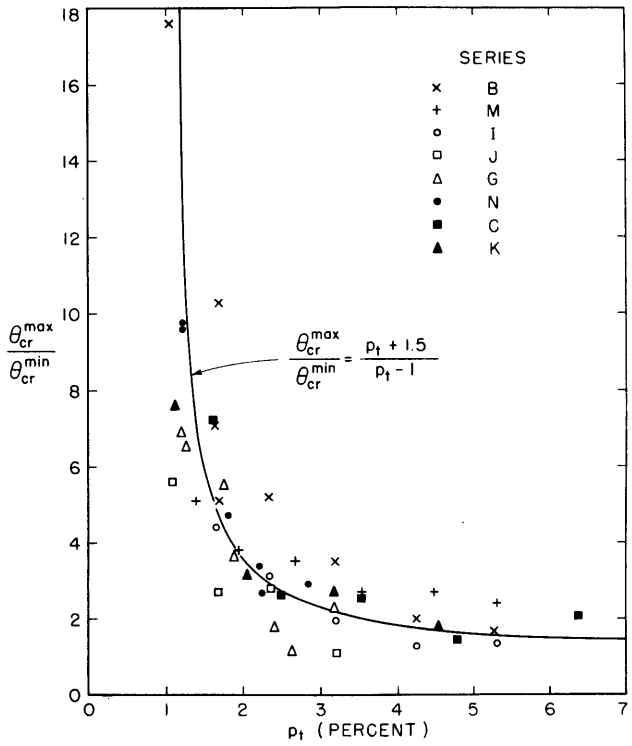

FIG. 10-21 $\theta_{cr}^{max}/\theta_{cr}^{min}$ AS A FUNCTION OF p_t

The crack pattern after failure for a typical Beam, B3, is shown in Fig. 10-22a. Cracks on the wider faces are inclined approximately 45 deg to the axis of the beam, except for a few cracks which turn to 90 deg at the edge. Cracks on the shorter face, however, are generally inclined at angles larger than 45 deg, and many of them are S-shaped with both ends of the cracks almost perpendicular to the edges. In other beams with large amounts of reinforcement, the cracks on the shorter faces at the failure location became numerous and random as shown in Fig. 10-22b.

The width and spacing of cracks are given in Table 10-7 at two load stages, one immediately after cracking and the other close to the ultimate torque. For the latter load stage, both the crack width and spacing are given; for the former stage only crack width is given. Both average and maximum crack width are given.

The crack widths and spacings were measured at the center of one wider face in the case of beams with four longitudinal corner bars only. However, for beams with six longitudinal bars, where the two additional bars were located at the center of the

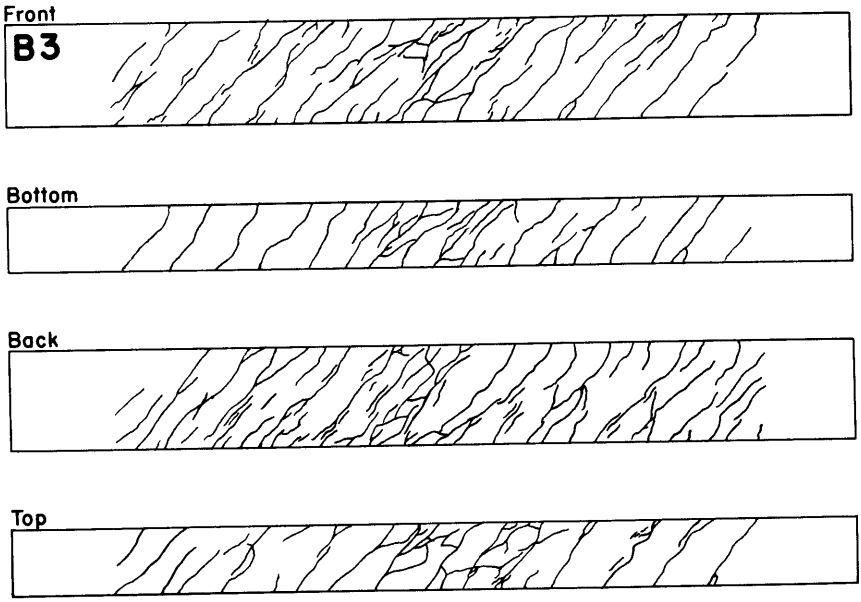

FIG. 10-22a CRACK PATTERN OF BEAM B3

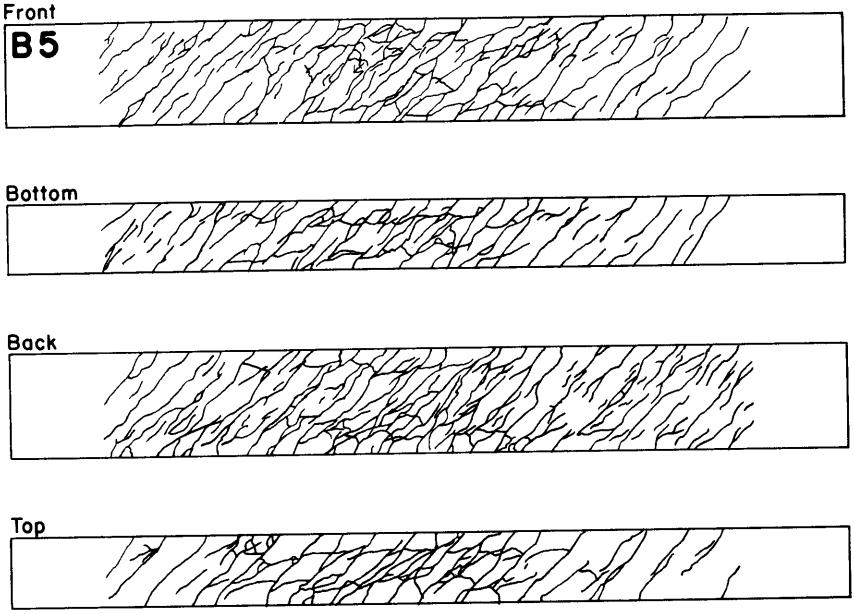

FIG. 10-22b CRACK PATTERN OF BEAM B5

TABLE 10-7 TEST RESULTS--CRACK WIDTH AND SPACING

Beam	Immediately After Cracking			One Load Stage Before T_u			
	Load, % of T_u	Crack Width, 10^{-3} in.		Load, % of T_u	Crack Width, 10^{-3} in.		Avg. Crack Spacing in.
		Avg.	Max.		Avg.	Max.	
B1	-	-	-	98	28	50	6.9
B2	68	13.0	17	96	18	31	6.0
B3	54	7.0	10	98	17	35	5.3
B4	48	4.2	6	96	6.8	12	3.7
B5	40	4.7	6	96	5.5	12	3.4
B6	42	3.5	5	97	5.0	10	3.2
B7	76	10.0	15	98	18	26	4.8
B8	67	2.7	6	97	4.3	10	3.2
B9	66	13.0	15	96	13	28	5.3
B10	57	3.7	6	95	23	37	6.9
D1	67	7.2	13	94	11.6	18	6.0
D2	57	7.0	10	92	9.0	15	4.8
D3	40	3.4	5	96	10.6	15	4.4
D4	37	3.1	5	96	7.3	20	3.4
M1	63	6.8	11	96	13.9	32	5.3
M2	51	5.0	9	96	9.3	28	2.8
M3	47	4.5	6	94	11.0	24	4.0
M4	42	2.3	4	94	7.0	14	3.0
M5	41	5.0	6	96	7.2	20	2.4
M6	39	1.8	3	98	8.2	25	2.3
I2	69	6.4	11	95	9.1	25	3.7
I3	56	5.4	8	95	7.4	18	3.4
I4	48	3.2	5	97	5.5	10	2.5
I5	45	3.6	6	98	6.4	12	2.4
I6	36	3.0	4	94	4.0	9	1.9
J1	66	10.5	12	92	11.9	29	4.8
J2	60	6.7	10	94	9.3	18	3.2
J3	56	4.2	7	92	6.3	22	2.5
J4	45	3.0	4	94	5.0	12	2.5
G1	-	-	-	-	-	-	-
G2	75	12.7	18	94	16.9	34	6.0
G3	59	10.7	14	97	13.1	28	4.0
G4	48	5.3	9	94	14.5	35	4.4
G5	42	3.4	5	95	5.6	14	3.4
G6	79	13.0	20	98	29.5	100	5.3
G7	64	5.1	10	96	10.1	25	3.2
G8	46	-	-	95	9.4	23	3.0
N1	84	12.7	22	94	19.4	55	5.1
N1a	79	10.4	15	94	13.6	20	4.0
N2	51	3.5	5	91	6.1	13	2.4
N2a	56	4.4	10	95	9.8	22	3.3
N3	62	4.5	7	96	8.3	17	2.8
N4	46	3.0	5	93	6.5	20	2.2
K1	83	8.2	16	92	9.7	20	3.0
K2	52	4.0	5	92	7.8	15	2.6
K3	45	3.0	4	90	7.5	15	2.7
K4	38	1.4	2	91	6.5	11	2.4
C1	-	-	-	-	-	-	-
C2	73	6.0	10	95	8.3	20	3.3
C3	61	3.0	4	94	7.9	20	2.8
C4	50	2.3	4	92	8.1	17	2.8
C5	47	1.3	2	91	3.7	7	2.0
C6	41	1.3	2	94	9.2	40	1.7

wider face, crack widths and spacings were also measured at the quarter-point of the wider face, because crack width at this location was often larger than at the center. The greater crack width at these two locations is recorded in Table 10-7.

In the typical Beam N2a, crack widths and spacings were measured at three locations--the center of the wider face, the center of the shorter face, and the edge of the wider face. Although crack spacings were approximately the same at these three locations, the crack width developed differently as shown in Fig. 10-23. Immediately after cracking, crack width was greatest at the center of the wider face, and widths at this location are recorded in Table 10-7. Crack widths at the center of the shorter face and at the edge of the wider face were less. The crack width at the first location increased approximately linearly with increasing torque, but those at the last two locations increased strongly with increasing torque. At the last load stage, 95 percent of ultimate, the maximum crack widths at the last two locations exceed that at the center of the wider face. Also, the surfaces at both sides of a crack at the corner were no longer in the same plane, showing that the longitudinal bars were subjected to dowel action. This dowel action was confirmed by measuring stresses on diametrically opposite faces of a longitudinal corner bar.

Table 10-7 shows that initial crack width was quite large for beams with small percentages of reinforcement. It decreased

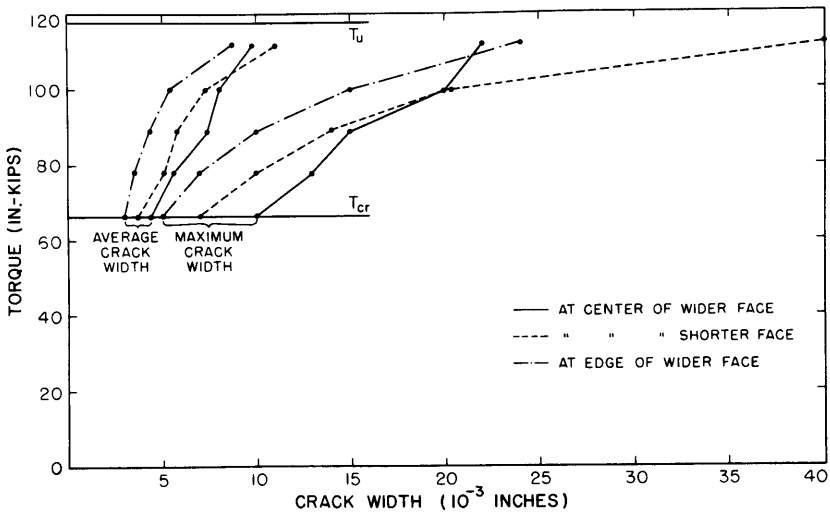

FIG. 10-23 INCREASE OF CRACK WIDTH WITH INCREASING TORQUE FOR BEAM N2a

rather rapidly, however, with increasing percentage of reinforcement. This is consistent with the observation that the twisting of beams under constant cracking torque, and the stresses in the reinforcement, also decrease with increasing percentage of reinforcement because the new equilibrium condition after cracking is reached earlier.

Length Increase of Torsional Beam After Cracking

An important phenomenon occurs after the cracking of concrete: The length of the beam increases with increasing torque. For example, the length change of Beam N2 was measured by two dial gages placed at both ends of the beam at the center of the cross-section. The torque versus unit lengthening diagram is shown in Fig. 10-24 by the solid curve. It shows that no significant change in length occurred before cracking. However, once the concrete cracked, the length of the beam began to increase with increasing torque. This lengthening was compared to the average measured strain of the longitudinal bars shown by the broken curve in Fig. 10-24. The correlation between lengthening of the beam and lengthening of the longitudinal bars is apparent.

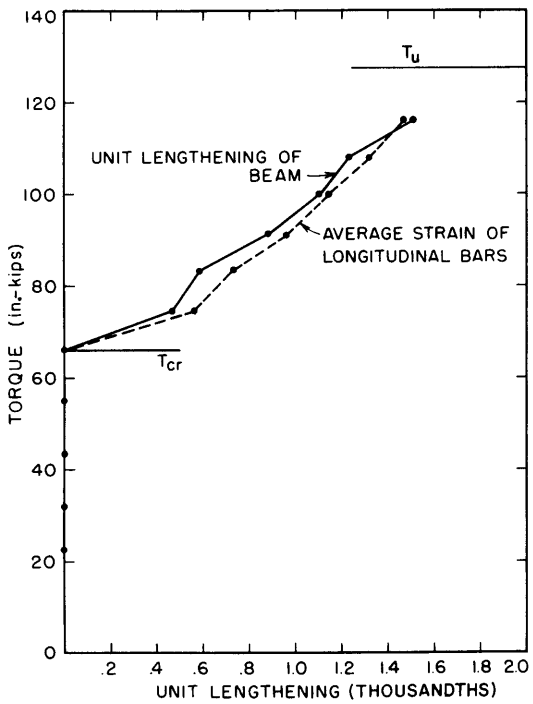

FIG. 10-24 INCREASE OF BEAM LENGTH WITH INCREASING TORQUE FOR BEAM N_2

This phenomenon has an important significance for torsional members restrained in the longitudinal direction, such as an edge beam in the center span of a multispan frame. Effects of this longitudinal restraint on the strength and behavior of the torsional beams deserve careful future research.

MAXIMUM AND MINIMUM PERCENTAGE OF REINFORCEMENT

It will be shown in a future paper that the ultimate torsional strength of an under-reinforced concrete beam can be predicted with sufficient accuracy by

$$T_u = \frac{2.4}{\sqrt{x}} x^2 y \sqrt{f'_c} + \left(0.66\ m + 0.33\ \frac{y_1}{x_1}\right)\frac{x_1 y_1 A_s f_{sy}}{s} \qquad (16)$$

in which $0.7 < m < 1.5$ and y_1/x_1 is taken as 2.6 whenever $y_1/x_1 > 2.6$. This equation was substantiated by 53 test beams reported herein and 27 test beams available in literature.

In order to use Eq. (16) the beams must be under-reinforced; i.e., the reinforcement must yield before compressive failure of concrete takes place. This criterion can be satisfied by limiting the maximum percentage of reinforcement, p_{tb}.

Test results and failure mechanism reveal that p_{tb} is approximately proportional to $\sqrt{f'_c}$ and inversely proportional to f_{sy}. Tests also show that the proportionality constant can be taken conservatively as 2400, and thus p_{tb} is proposed to be limited by

$$p_{tb} = 2400\ \frac{\sqrt{f'_c}}{f_{sy}} \qquad (17)$$

where f'_c and f_{sy} are in psi and p_{tb} in percent.

It must be mentioned that p_{tb} is also a function of m and y_1/x_1. However, these effects were neglected because of insufficient data, and also because they appear to be small in comparison with f'_c and f_{sy}.

The purpose of reinforcing a concrete beam is to increase the ultimate strength and to gain a ductile behavior before failure. These purposes can be accomplished by specifying a minimum amount of reinforcement in the beams to develop an ultimate strength larger than the failure torque of the corresponding plain concrete beam; i.e.,

$$T_u > T_{up} \qquad (18)$$

Substituting T_u from Eq. (16) and T_{up} from Eq. (1a) into this equation and rearranging the terms, the minimum amount of reinforcement is:

$$\frac{A_s}{s} x_1 y_1 f_{sy} = \frac{6(x^2 + 10)\, y \sqrt[3]{f'_c} - \frac{2.4}{\sqrt{x}} x^2 y \sqrt{f'_c}}{0.66\, m + 0.33 \frac{y_1}{x_1}} \tag{19}$$

This reinforcement requirement can be defined in terms of volume percentage of reinforcement as follows: The steel volume of a single stirrup is $2(x_1 + y_1)\, A_s$, and the total beam volume occupied by one stirrup is xys. Thus, the volume percentage of stirrups, p_s, is

$$p_s = \frac{2(x_1 + y_1)}{xy} \cdot \frac{A_s}{s} \cdot 100$$

Substituting for A_s/s as defined by Eq. (19), p_s becomes

$$p_s = \frac{2x(x_1 + y_1)\left[6\left(1 + \frac{10}{x^2}\right)\sqrt[3]{f'_c} - \frac{2.4}{\sqrt{x}}\sqrt{f'_c}\right]}{x_1 y_1 f_{sy}\left(0.66\, m + 0.33 \frac{y_1}{x_1}\right)} \cdot 100 \tag{20}$$

The volume percentage of longitudinal reinforcement is

$$p_\ell = m\, p_s$$

and the total volume percentage of reinforcement is

$$p_t = p_\ell + p_s = (1 + m)\, p_s$$

Eq. (19) and Eq. (20) are rather lengthy. For practical purposes one might as well calculate T_u and T_{up} separately to see if they satisfy Eq. (18). As a guide, however, the minimum percentage of stirrups is 0.5 percent, and the minimum percentage of total reinforcement, p_t, is 1 percent.

CONCLUSIONS

Fifty-three reinforced concrete beams with longitudinal bars and closed stirrups were subjected to pure torsion in a systematic investigation of the effect of eight variables.

The behavior of a reinforced concrete beam subjected to torsion is very different before and after cracking. The cracking torque is $(1 + 0.04\, p_t)$ times the failure torque of the corresponding

plain concrete beam, in which p_t is the total volume of reinforcement expressed in percent.

Before cracking, the behavior of a reinforced concrete beam is identical to its corresponding plain concrete beam with no effect from the reinforcement. The torsional stiffness can be taken as the ratio of the failure torque over the angle of twist at failure of the corresponding plain concrete beam (T_{up}/θ_{up}).

After cracking, the behavior of a reinforced concrete beam is completely different from that predicted by Saint-Venant's theory. The stresses in the longitudinal bars and stirrups do not follow Saint-Venant's distribution. The principal compressive strain is much larger than that predicted. Also, the length of the beam increases with increasing torque because of lengthening of the longitudinal bars.

Reinforced concrete beams can be divided into under-reinforced beams, in which the reinforcement yields before compressive crushing of the concrete, and over-reinforced beams, in which the concrete fails before yielding of the steel. The maximum percentage of reinforcement which ensures that a beam will be under-reinforced is given by an empirical equation.

The balanced ratio of volume of longitudinal bars to volume of stirrups, which ensures that both types of reinforcement will yield at failure, is not always unity. Ratios other than the balanced ratio will result in partially over-reinforced beams, in which either longitudinal bars or stirrups do not yield at failure.

For under-reinforced beams, ultimate torque can be expressed satisfactorily in two terms:

$$T_o + \Omega x_1 y_1 \frac{A_s f_{sy}}{s},$$

which is the form derived by Rausch and Cowan. However, Rausch and Cowan's theory (the German Code and Australian Code, respectively) were found to be unconservative. Similarly, Lessig's theory (or the Russian Code) is also unconservative.

The concrete core of a reinforced concrete beam does not contribute to the ultimate resistance of the solid beam. The term T_o is not contributed by the concrete core.

The value of Ω is not a constant. It is a function of m (ratio of volume of longitudinal bars to volume of stirrups), y_1/x_1 (ratio of larger to smaller dimension of closed stirrups), the scale and other smaller effects such as spacing of stirrups and concrete strength.

Empirical equations are given for angle of twist at ultimate torque and at cracking torque, and for torsional stiffness after cracking.

ACKNOWLEDGMENTS

This investigation was carried out in the Structural Laboratory of the Portland Cement Association under the direction of Dr. Eivind Hognestad. Contributions to the laboratory work were also made by O. A. Kurvits, W. W. Berglund, R. K. Richter, and W. Hummerich, Jr., of the technician staff. Acknowledgment is also made to Professor Alan H. Mattock, formerly with the PCA Laboratories and now with the University of Washington.

REFERENCES

1. Hsu, T. T. C., and Mattock, A. H., "A Torsion Test Rig," Journal, PCA Research and Development Laboratories, V. 7, No. 1, Jan. 1965, pp. 2-9; also Bulletin D91, PCA Development Department.

2. Hsu, T. T. C., "Torsion of Structural Concrete - Plain Concrete Rectangular Sections," Torsion of Structural Concrete, Special Publication No. 18, American Concrete Institute, Detroit, 1968.

3. Rausch, E., "Drillung, Schub und Scheren im Stahlbetonbau" (Torsion, Diagonal Tension and Shear in Reinforced Concrete), Deutscher Ingenieur-Verlag Gmbh, Düsseldorf, 1953, 168 pp.

4. Cowan, H. J., "Design of Beams Subjected to Torsion Related to the New Australian Code," ACI JOURNAL, Proceedings V. 56, No. 7, Jan. 1960, pp. 591-618.

5. "Bemessung im Stahlbetonbau," (Design of Reinforced Concrete), DIN 4224, German Standard, Wilhelm Ernst and Sohn, Berlin, 1958, 57 pp.

6. "SAA Code for Concrete in Buildings," Australian Standard No. CA. 2-1958, Standards Association of Australia, Sydney, 1958, 109 pp.

7. Lessig, N. N., "Determination of Load Carrying Capacity of Reinforced Concrete Element with Rectangular Cross-Section Subjected to Flexure with Torsion," Concrete and Reinforced Concrete Institute, Trudy, No. 5, 1959, pp. 5-28. (in Russian).

8. "Structural Standards and Regulations, Part II, Section B," State Committee on Construction, USSR Council of Ministers, Moscow, 1962, 100 pp.

NOTATION

A_ℓ = cross-sectional area of one longitudinal bar

$\overline{A}_\ell$ = cross-sectional area of one-half of the total longitudinal bars

A_s = cross-sectional area of one stirrup leg

C = an empirical constant

f'_c = cylinder compressive strength of concrete

f_r = modulus of rupture of concrete

f_{sp} = split-cylinder tensile strength of concrete

f_t = uniaxial tensile strength of concrete

$f_{\ell y}$ = yield strength of longitudinal bars

f_{sy} = yield strength of stirrups

G = modulus of rigidity of concrete

K_t = torsional stiffness before cracking

K_{tcr} = torsional stiffness after cracking

m = ratio of volume of longitudinal bars to volume of stirrups

m_b = balanced ratio of volume of longitudinal bars to volume of stirrups

p_ℓ = volume percentage of longitudinal bars

p_s = volume percentage of stirrups

p_t = total volume percentage of reinforcement

p_{tb} = balanced total volume percentage of reinforcement

S = slope in the T/T_{up} versus θ/θ_{up} diagram

s = spacing of stirrups in the direction parallel to the longitudinal axis of beams

s_{max} = maximum spacing of stirrups

T = externally applied torque

T_{cr} = cracking torque of reinforced concrete members

T_o = T_u-intercept of a T_u versus $x_1 y_1 A_s f_{sy}/s$ curve

T_u = ultimate torque of reinforced concrete beams

T_{up} = ultimate torque of plain concrete beams

x = smaller over-all dimension of rectangular cross-section

x_1 = smaller center-to-center dimension of a closed rectangular stirrup

y = larger over-all dimension of rectangular cross-section

y_1 = larger center-to-center dimension of a closed rectangular stirrup

β = Saint-Venant's coefficient, which is a function of y/x

ε_{cr} = principal compressive strain of concrete measured at the center of wider face immediately before cracking

ε_{u} = principal compressive strain of concrete measured at the center of wider face at ultimate torque

θ = angle of twist (radian/in. or deg/in.)

θ_{cr} = experimental angle of twist immediately before cracking

θ_{cr}^{min} = minimum angle of twist at cracking torque, defined by Eq. (14)

θ_{cr}^{max} = maximum angle of twist at cracking torque

θ_{u} = angle of twist at ultimate torque of reinforced concrete members (radian/in. or deg/in.)

θ_{up} = angle of twist at failure of plain concrete members

Ω = slope of a T_u versus $x_1 y_1 A_s f_{sy}/s$ curve